



THE UNIVERSITY OF  
**WAIKATO**  
*Te Whare Wānanga o Waikato*

Research Commons

<http://waikato.researchgateway.ac.nz/>

## Research Commons at the University of Waikato

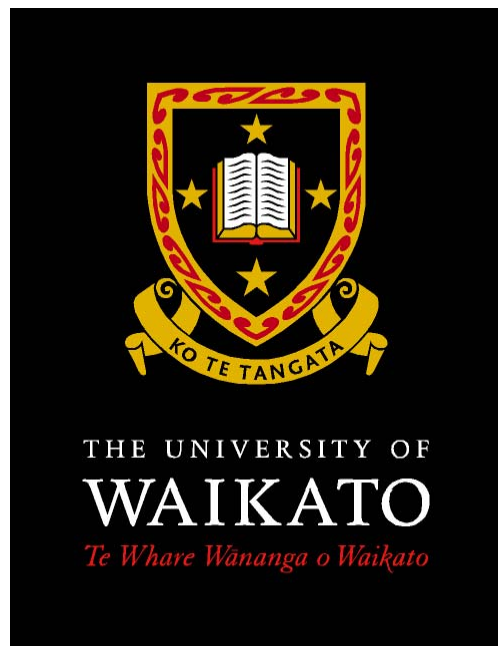
### Copyright Statement:

The digital copy of this thesis is protected by the Copyright Act 1994 (New Zealand).

The thesis may be consulted by you, provided you comply with the provisions of the Act and the following conditions of use:

- Any use you make of these documents or images must be for research or private study purposes only, and you may not make them available to any other person.
- Authors control the copyright of their thesis. You will recognise the author's right to be identified as the author of the thesis, and due acknowledgement will be made to the author where appropriate.
- You will obtain the author's permission before publishing any material from the thesis.

*Bounded Eigenvalues of Fully  
Clamped and Completely Free  
Rectangular Plates*



A thesis submitted in total fulfillment  
of the requirements for the degree of  
Masters of Engineering  
In Mechanical Engineering  
by

**Yusuke Mochida**

The University of Waikato  
Hamilton, New Zealand

2007

## **Abstract**

Exact solution to the vibration of rectangular plates is available only for plates with two opposite edges subject to simply supported conditions. Otherwise, they are analysed by using approximate methods. There are several approximate methods to conduct a vibration analysis, such as the Rayleigh-Ritz method, the Finite Element Method, the Finite Difference Method, and the Superposition Method. The Rayleigh–Ritz method and the finite element method give upper bound results for the natural frequencies of plates. However, there is a disadvantage in using this method in that the error due to discretisation cannot be calculated easily. Therefore, it would be good to find a suitable method that gives lower bound results for the natural frequencies to complement the results from the Rayleigh-Ritz method. The superposition method is also a convenient and efficient method but it gives lower bound solution only in some cases. Whether it gives upper bound or lower bound results for the natural frequencies depends on the boundary conditions. It is also known that the finite difference method always gives lower bound results. This thesis presents bounded eigenvalues, which are dimensionless form of natural frequencies, calculated using the superposition method and the finite difference method. All computations were done using the MATLAB software package. The convergence tests show that the superposition method gives a lower bound for the eigenvalues of fully clamped plates, and an upper bound for the completely free plates. It is also shown that the finite difference method gives a lower bound for the eigenvalues of completely free plates. Finally, the upper bounds and lower bounds for the eigenvalues of fully clamped and completely free plates are given.

## **Acknowledgement**

The author would like to acknowledge the direction, guidance and advice by Associate Professor Sinniah Ilanko with respect of this thesis.

He would also like to thank his family in their total support.

## Table of Contents

Abstract .....	i
Acknowledgement .....	ii
Table of Contents .....	iii
Table of Figures .....	iv
List of Tables .....	vi
Nomenclature .....	vii
<b>1. INTRODUCTION .....</b>	<b>2</b>
1.1. Vibration of plate .....	2
1.2. Project scope .....	2
<b>2. BACKGROUND THEORY .....</b>	<b>5</b>
2.1. The Superposition Method .....	6
2.1.1. Fully Clamped Plate .....	6
2.1.2. Completely Free Plate .....	14
2.2. The Finite Difference Method .....	21
2.2.1. Fully Clamped plate .....	24
2.2.2. Completely Free Plate .....	25
<b>3. NUMERICAL RESULTS .....</b>	<b>28</b>
3.1. The Superposition Method .....	28
3.1.1. Fully Clamped Plate .....	28
3.1.2. Completely Free Plate .....	36
3.2. The Finite Difference Method .....	43
3.2.1. Completely Free Plate .....	43
<b>4. DISCUSSION .....</b>	<b>52</b>
4.1. Fully Clamped Plate .....	52
4.2. Completely Free Plate .....	54
<b>5. CONCLUSION and RECOMMENDATIONS .....</b>	<b>58</b>
References .....	60
Appendix I: Theory of Thin Rectangular Plate .....	61

## Table of Figures

Figure 2.1 A quarter segment of the plate.....	6
Figure 2.2 Building blocks used to analyse the doubly symmetric mode of fully clamped plates.....	7
Figure 2.3 Building blocks used to analyse the doubly antisymmetric mode of fully clamped plates .....	10
Figure 2.4 Building blocks used to analyse the symmetric- antisymmetric mode of fully clamped plates .....	12
Figure 2.5 Building blocks used to analyse the fully symmetric mode of the completely free plate.....	14
Figure 2.6 Building blocks used to analyse the fully antisymmetric mode of the completely free plate.....	17
Figure 2.7 Building blocks used to analyse the symmetric-antisymmetric mode of the completely free plate.....	19
Figure 2.8 The F.D. Scheme for a plate (a) the mesh and a typical node and (b) the F. D. molecular formula.....	22
Figure 2.9 The node distribution at the edge of a fully clamped plate.....	24
Figure 2.10 The node distribution for a completely free plate: (a) at the edge; (b) at the corner.....	25
Figure 3.1 Convergence test for the eigenvalues of fully clamped rectangular plate computed by the superposition method ( $\Phi = 1.0$ ).....	30
Figure 3.2 Convergence test for the eigenvalues of fully clamped rectangular plate computed by the superposition method ( $\Phi = 1.25$ ).....	31
Figure 3.3 Convergence test for the eigenvalues of fully clamped rectangular plate computed by the superposition method ( $\Phi = 1.5$ ).....	32
Figure 3.4 Convergence test for the eigenvalues of fully clamped rectangular plate computed by the superposition method ( $\Phi = 2.0$ ).....	33
Figure 3.5 Convergence test for the eigenvalues of fully clamped rectangular plate computed by the superposition method ( $\Phi = 2.5$ ).....	34
Figure 3.6 Convergence test for the eigenvalues of fully clamped rectangular plate computed by the superposition method ( $\Phi = 3.0$ ).....	35

Figure 3.7 Convergence test for the eigenvalues of completely free rectangular plate computed by the superposition method ( $\Phi = 1.0$ ) .....	37
Figure 3.8 Convergence test for the eigenvalues of completely free rectangular plate computed by the superposition method ( $\Phi = 1.25$ ) .....	38
Figure 3.9 Convergence test for the eigenvalues of completely free rectangular plate computed by the superposition method ( $\Phi = 1.5$ ) .....	39
Figure 3.10 Convergence test for the eigenvalues of completely free rectangular plate computed by the superposition method ( $\Phi = 2.0$ ) .....	40
Figure 3.11 Convergence test for the eigenvalues of completely free rectangular plate computed by the superposition method ( $\Phi = 2.5$ ) .....	41
Figure 3.12 Convergence test for the eigenvalues of completely free rectangular plate computed by the superposition method ( $\Phi = 3.0$ ) .....	42
Figure 3.13 Convergence test for the eigenvalues of completely free rectangular plate computed by the finite difference method ( $\Phi = 1.0$ ) .....	45
Figure 3.14 Convergence test for the eigenvalues of completely free rectangular plate computed by the finite difference method ( $\Phi = 1.25$ ) .....	46
Figure 3.15 Convergence test for the eigenvalues of completely free rectangular plate computed by the finite difference method ( $\Phi = 1.5$ ) .....	47
Figure 3.16 Convergence test for the eigenvalues of completely free rectangular plate computed by the finite difference method ( $\Phi = 2.0$ ) .....	48
Figure 3.17 Convergence test for the eigenvalues of completely free rectangular plate computed by the finite difference method ( $\Phi = 2.5$ ) .....	49
Figure 3.18 Convergence test for the eigenvalues of completely free rectangular plate computed by the finite difference method ( $\Phi = 3.0$ ) .....	50

## List of Tables

Table 3.1 The eigenvalues of fully clamped plates obtained by the superposition method ( $\lambda^2 = \omega a^2 \sqrt{\rho/D}$ ). .....	29
Table 3.2 The eigenvalues of completely free plates obtained by the superposition method ( $\lambda^2 = \omega a^2 \sqrt{\rho/D}$ , $\nu = 0.3$ ). .....	36
Table 3.3 The eigenvalues of completely free plates obtained by the superposition method ( $\lambda^2 = \omega a^2 \sqrt{\rho/D}$ , $\nu = 0.3$ ). .....	44
Table 4.1 The lower bound and the upper bound for the eigenvalues of fully clamped rectangular plates with an aspect ratio of 1:3 ( $\lambda^2 = \omega a^2 \sqrt{\rho/D}$ ) [8], ....	53
Table 4.2 The lower bound and the upper bound for the eigenvalues of completely free rectangular plates with an aspect ratio of 1:3. ....	55
Table 4.3 Comparison of eigenvalues obtained by the FDM with those in Leissa's monograph [1] for the doubly antisymmetric modes of the square free plate ( $\nu = 0.3$ ) .....	56

## Nomenclature

$a$	plate dimension in $x$ direction
$b$	plate dimension in $y$ direction
$m$	mass per unit area of plate
$h$	plate thickness
$q$	transverse static loading
$w$	plate lateral deflection
$x, y$	plate spatial co-ordinates
$D$	plate flexural rigidity, $(Eh/12)/(1-\nu^2)$
$E$	modulus of elasticity of material
$K_f$	number of terms in Fourier expansions
$P$	the number of nodes in $x$ direction
$Q$	the number of nodes in $y$ direction
$H$	mesh size parallel to $x$ direction, $a/(P-1)$
$K$	mesh size parallel to $y$ direction, $b/(Q-1)$
$M$	bending moment distributed along edge of plate
$V$	plate vertical edge reaction
$\xi$	dimensionless plate spatial co-ordinates $x/a$
$\eta$	dimensionless plate spatial co-ordinates $y/b$
$\rho$	mass per unit area of plate
$\omega$	radian frequency of vibration
$\Phi$	aspect ratio of the plate $b/a$
$\nu$	Poisson's ratio of material
$\nu^*$	$2-\nu$
$\lambda^2$	$\omega a^2 \sqrt{\rho / D}$
$\lambda^{*2}$	$\omega b^2 \sqrt{\rho / D}$

# **Chapter I**

## **Introduction**

# 1. INTRODUCTION

## ***1.1. Vibration of plate***

The rectangular plate is one of the most common components in engineering machines and structures, for example, bridges, buildings or airplane wings. In many design problems, static analysis of the plates alone is insufficient. Rather, their design needs to include the effects of periodic or random time varying forces causing vibration.

It is well known that there are a number of discrete frequencies at which rectangular plates will oscillate with large displacements. They are called natural frequencies of the plate. It is also known that there is a characteristic shape associated with each natural frequency. It is called a modal shape or mode.

When periodic or random driving forces exist on the plate, and if the frequency of excitation coincides with one of the natural frequencies of the plate, a condition of resonance is encountered, and critically large oscillations that cause the failure of structures may occur. Thus it is essential for the designer to conduct an accurate vibration analysis of rectangular plates to determine the natural frequencies, modes and the dynamic response.

## ***1.2. Project scope***

A rectangular plate can have 21 combinations of classical boundary conditions, i.e. either clamped, simply supported or free. These can be divided into two groups in respect of the boundary conditions. The first group is the plates with at least two opposite edges simply supported. The second group is the plates which do not have a pair of opposite edges simply supported. The first group of problems have exact solutions. The other, including fully clamped and completely free rectangular plates, are analysed by using approximate methods, for example

the Rayleigh-Ritz method, because functions which simultaneously satisfy the governing differential equation and the boundary conditions have not yet been found. An excellent review of the literature relating to vibration analysis of plates was published by Leissa [1].

Most of these methods give upper bounds for the eigenvalues as the solution is based on assumed shapes which effectively overconstrain the system. The most popular method, namely the Rayleigh–Ritz method gives upper bound results for the natural frequencies. However there is a disadvantage in relying on this method alone, in that the error due to discretisation cannot be calculated easily. Therefore, it would be good to investigate other methods which give a lower bound result and thus complement those upper bound results.

Gorman has conducted free vibration analysis of fully clamped plate and completely free plate by the method of superposition [2]. The superposition method is very efficient and appears to give the best values for the natural frequencies of plates with various aspect ratios. [3, 4]. A recent publication predicts that the superposition method would give an upper bound or a lower bound result depending on whether the boundary conditions of the building blocks are stiffer or more flexible than those of the actual system [4].

The Finite Difference Method (FDM) is traditionally used to solve the static and dynamic problems of plates. It gives a lower bound for the eigenvalues [5].

The purpose of this thesis is to numerically verify the prediction in the recent publication [4] and also to obtain upper bound and lower bound values for the natural frequencies of fully clamped and completely free rectangular plates with various aspect ratios using the superposition method and the finite difference method.

# **Chapter II**

## **Background Theory**

## 2. BACKGROUND THEORY

The partial differential equation governing the out-of-plane vibration of rectangular plates is

$$\frac{\partial^4 W(x, y)}{\partial x^4} + 2 \frac{\partial^4 W(x, y)}{\partial x^2 \partial y^2} + \frac{\partial^4 W(x, y)}{\partial y^4} - \frac{\rho \omega^2}{D} W(x, y) = 0 \quad (2.1)$$

For convenience, the governing equation is expressed in dimensionless form. Gorman [2] uses dimensionless coordinates  $\xi$  and  $\eta$ , where  $\xi = x/a$ ,  $\eta = y/b$ , in which  $a$  and  $b$  are the plate dimensions. The equation may be then written as

$$\frac{\partial^4 W(\xi, \eta)}{\partial \eta^4} + 2\Phi^2 \frac{\partial^4 W(\xi, \eta)}{\partial \eta^2 \partial \xi^2} + \Phi^4 \left\{ \frac{\partial^4 W(\xi, \eta)}{\partial \xi^4} - \lambda^4 W(\xi, \eta) \right\} = 0 \quad (2.2)$$

where  $\lambda^2 = \omega a^2 \sqrt{\rho/D}$  and  $\Phi$  is the plate aspect ratio  $b/a$ .

The bending moment distributed the edges perpendicular to the  $\xi$  axis or the  $\eta$  axis is expressed as follows

$$\frac{b^2 M(\xi)}{aD} = - \left[ \frac{\partial^2 W(\xi, \eta)}{\partial \eta^2} + \nu \Phi^2 \frac{\partial^2 W(\xi, \eta)}{\partial \xi^2} \right] \quad (2.3)$$

and

$$\frac{aM(\eta)}{D} = - \left[ \frac{\partial^2 W(\xi, \eta)}{\partial \xi^2} + \frac{\nu}{\Phi^2} \frac{\partial^2 W(\xi, \eta)}{\partial \eta^2} \right] \quad (2.4)$$

The vertical edge reaction along the edges perpendicular to the  $\xi$  axis and the  $\eta$  axis are expressed as follows

$$\frac{b^3 V(\xi)}{aD} = - \left[ \frac{\partial^3 W(\xi, \eta)}{\partial \eta^3} + \nu^* \Phi^2 \frac{\partial^3 W(\xi, \eta)}{\partial \eta \partial \xi^2} \right] \quad (2.5)$$

and

$$\frac{a^2 V(\eta)}{D} = - \left[ \frac{\partial^3 W(\xi, \eta)}{\partial \xi^3} + \frac{\nu^*}{\Phi^2} \frac{\partial^3 W(\xi, \eta)}{\partial \xi \partial \eta^2} \right] \quad (2.6)$$

## 2.1. The Superposition Method

The development of the eigenvalue matrix for fully clamped plates and completely free plates by using the superposition method are described in an earlier literature [2]. The derivations for the application of the superposition method in this thesis are taken from the same reference and are therefore based on quarter plate dimension shown in Figure 2.1. In the superposition method, two or more plate problems which have exact solutions are considered. The plate problems are often referred to as building blocks. In order to solve the original plate problems, these building blocks are superimposed and constants existing in the equations of motion of them are changed so that their combination satisfies the boundary conditions of original plate problems.

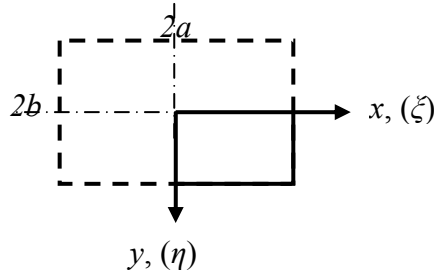


Figure 2.1 A quarter segment of the plate

### 2.1.1. Fully Clamped Plate

Modes of free vibration of the plate may be categorised into the following three types depending on the nature of the modes: (a) the modes fully symmetric about the  $x$  (or  $\xi$ ) axis and the  $y$  (or  $\eta$ ) axis; (b) the modes fully antisymmetric about both axes; (c) the modes symmetric about the  $x$  axis and antisymmetric about the  $y$  axis or vice versa.

#### *Doubly Symmetric Mode*

Firstly, to solve the fully symmetric mode problem, only a quarter of the fully clamped plate needs to be considered as shown in Figure 2.1. The original fully clamped plate would have dimensions  $2a \times 2b$  so that the dimensions of the

quarter segment would be  $a \times b$ . The building blocks used for the doubly symmetric modes in the superposition method are depicted in Figure 2.2. The edges  $\xi = 1$  and  $\eta = 1$  have simple support conditions and are subjected to bending moment  $M_1(\xi)$  or  $M_2(\eta)$ . The edges  $\xi = 0$  and  $\eta = 0$  with two small circles imply slip shear condition, which means no vertical edge reaction and no slope taken normal to the edge.

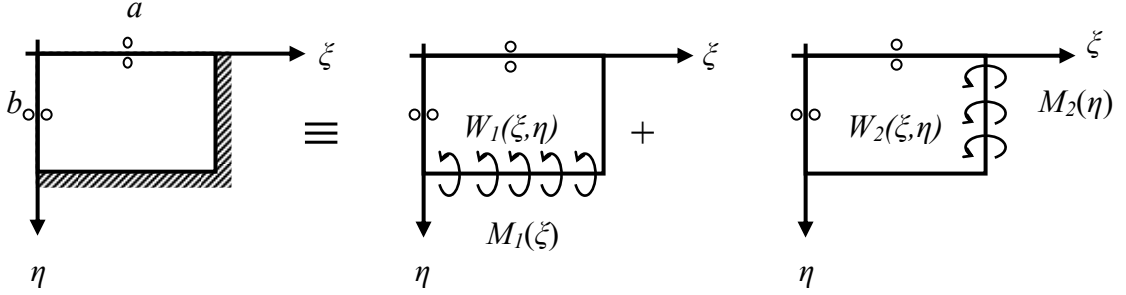


Figure 2.2 Building blocks used to analyse the doubly symmetric mode of fully clamped plates

For the first and second building block, their solutions may have Lévy type solution expressed as

$$W_1(\xi, \eta) = \sum_{m=1,3,5}^{\infty} Y_m(\eta) \cos \frac{m\pi\xi}{2} \quad (2.7)$$

and

$$W_2(\xi, \eta) = \sum_{n=1,3,5}^{\infty} Y_n(\xi) \cos \frac{n\pi\eta}{2} \quad (2.8)$$

Substituting Equation 2.7 into Equation 2.2 one obtains

$$\frac{d^4 Y_m(\eta)}{d\eta^4} + 2\Phi^2 \left( \frac{m\pi}{2} \right)^2 \frac{d^2 Y_m(\eta)}{d\eta^2} + \Phi^4 \left\{ \left( \frac{m\pi}{2} \right)^4 - \lambda^4 \right\} Y_m(\eta) = 0 \quad (2.9)$$

The solution to Equation 2.9 depends on whether the eigenvalue  $\lambda^2$  is greater than or less than  $(m\pi/2)^2$ . The typical solutions that satisfy Equation 2.9 for  $\lambda^2 > (m\pi/2)^2$  are

$$Y_m(\eta) = A_m \sinh \beta_m \eta + B_m \cosh \beta_m \eta + C_m \sin \gamma_m \eta + D_m \cos \gamma_m \eta \quad (2.10)$$

and for  $\lambda^2 < (m\pi/2)^2$ ,

$$Y_m(\eta) = A_m \sinh \beta_m \eta + B_m \cosh \beta_m \eta + C_m \sinh \gamma_m \eta + D_m \cosh \gamma_m \eta \quad (2.11)$$

where  $\beta_m = \Phi\sqrt{\lambda^2 + (m\pi/2)^2}$  and  $\gamma_m = \Phi\sqrt{\lambda^2 - (m\pi/2)^2}$  for  $\lambda^2 > (m\pi/2)^2$  or  $\gamma_m = \Phi\sqrt{(m\pi/2)^2 - \lambda^2}$  for  $\lambda^2 < (m\pi/2)^2$ . Here,  $A_m$ ,  $B_m$ ,  $C_m$ , and  $D_m$  are constants to be determined.

Now, only symmetric terms will remain because of symmetry about the  $\zeta$  axis. Two coefficients are, therefore, eliminated. The other two coefficients are determined by enforcing the condition of zero displacement and the equilibrium of moment along the edge  $\eta = l$ . It is considered that the bending moment distributed along the edge should fluctuate sinusoidally with the same frequency as the vibrating plate. The bending moment  $M_l(\zeta)$  could be expressed by the following Fourier expansion

$$\frac{b^2 M_l(\zeta)}{aD} = \sum_{m=1,3,5,\dots}^{\infty} E_m \cos \frac{m\pi\zeta}{2} \quad (2.12)$$

Substituting Equation 2.7 into Equation 2.3, the boundary condition of equilibrium of moment at along the edge  $\eta = l$  can be written as

$$\frac{\partial^2}{\partial \eta^2} \left[ Y_m(\eta) \cos \frac{m\pi\zeta}{2} \right] + \nu \Phi^2 \frac{\partial^2}{\partial \zeta^2} \left[ Y_m(\eta) \cos \frac{m\pi\zeta}{2} \right]_{\eta=l} = -E_m \cos \frac{m\pi\zeta}{2} \quad (2.13)$$

Since derivatives of  $W(\zeta, \eta)$  with respect to  $\zeta$  are zero along the edge  $\eta = l$ , Equation 2.13 can be simplify to

$$\left. \frac{\partial^2 Y_m(\eta)}{\partial \eta^2} \right|_{\eta=l} = -E_m \quad (2.14)$$

The analytical function  $Y_m(\eta)$  for  $\lambda^2 > (m\pi/2)^2$  may be written as,

$$Y_m(\eta) = E_m (\theta_{m11} \cosh \beta_m \eta + \theta_{m12} \cos \gamma_m \eta) \quad (2.15)$$

where,

$$\theta_{m11} = \frac{-1.0}{(\beta_m^2 + \gamma_m^2) \cosh \beta_m}, \text{ and } \theta_{m12} = \frac{1.0}{(\beta_m^2 + \gamma_m^2) \cos \gamma_m}$$

and for  $\lambda^2 < (m\pi/2)^2$ ,

$$Y_m(\eta) = E_m (\theta_{m21} \cosh \beta_m \eta + \theta_{m22} \cosh \gamma_m \eta) \quad (2.16)$$

where,

$$\theta_{m21} = \frac{-1.0}{(\beta_m^2 - \gamma_m^2) \cosh \beta_m}, \text{ and } \theta_{m22} = \frac{1.0}{(\beta_m^2 - \gamma_m^2) \cosh \gamma_m}$$

Next, for the second building block, the analytical function,  $Y_n(\xi)$ , can be easily obtained from the first building block by interchange of coordinates due to symmetry. However, the aspect ratio must be replaced by its inverse and  $\lambda^2$  must be multiplied by  $\Phi^2$ . The analytical functions of the second building block are expressed as follows.

For  $\Phi^2\lambda^2 > (n\pi/2)^2$

$$Y_n(\xi) = E_n (\theta_{n11} \cosh \beta_n \xi + \theta_{n12} \cos \gamma_n \xi) \quad (2.17)$$

where,

$$\theta_{n11} = \frac{-1.0}{(\beta_n^2 + \gamma_n^2) \cosh \beta_n}, \text{ and } \theta_{n12} = \frac{1.0}{(\beta_n^2 + \gamma_n^2) \cos \gamma_n}$$

and, for  $\Phi^2\lambda^2 < (n\pi/2)^2$ ,

$$Y_n(\xi) = E_n (\theta_{n21} \cosh \beta_n \xi + \theta_{n22} \cosh \gamma_n \xi) \quad (2.18)$$

where,

$$\theta_{n21} = \frac{-1.0}{(\beta_n^2 - \gamma_n^2) \cosh \beta_n}, \text{ and } \theta_{n22} = \frac{1.0}{(\beta_n^2 - \gamma_n^2) \cosh \gamma_n}$$

$$\beta_n = (1/\Phi) \sqrt{\lambda^2 \Phi^2 + (n\pi/2)^2}$$

and

$$\gamma_n = (1/\Phi) \sqrt{\lambda^2 \Phi^2 - (n\pi/2)^2} \text{ or } \gamma_n = (1/\Phi) \sqrt{(n\pi/2)^2 - \lambda^2 \Phi^2} \text{ whichever is real.}$$

### ***Doubly Antisymmetric Mode***

A different set of building blocks will be considered when analysing different vibration modes. For fully antisymmetric modes, for example, slip-shear conditions must be replaced by simple support conditions along the  $\xi$  and  $\eta$  axes as shown in Figure 2.3. In such case, the displacement functions  $W_1$  and  $W_2$  may be expressed as

$$W_1(\xi, \eta) = \sum_{m=1,2}^{\infty} Y_m(\eta) \sin m\pi\xi \quad (2.19)$$

and

$$W_2(\xi, \eta) = \sum_{n=1,2}^{\infty} Y_n(\xi) \sin n\pi\eta \quad (2.20)$$

respectively.

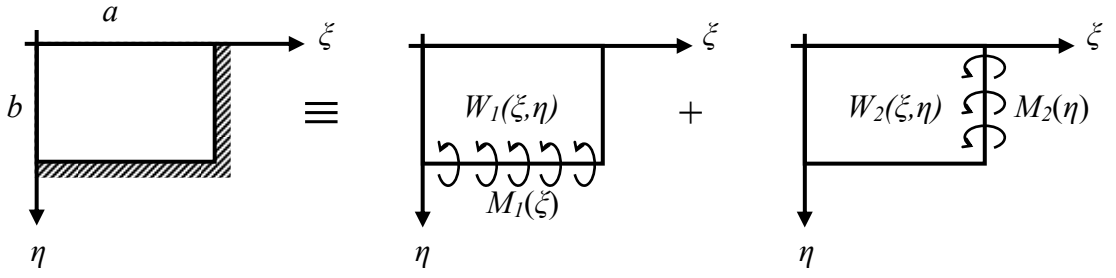


Figure 2.3 Building blocks used to analyse the doubly antisymmetric mode of fully clamped plates

Similar to the doubly symmetric case, the bending moment distributed along the edge  $\xi = l$  and the edge  $\eta = l$  are expanded in series form as

$$\frac{b^2 M_1(\xi)}{aD} = \sum_{m=1,2,\dots}^{\infty} E_m \sin m\pi\xi \quad (2.21)$$

and

$$\frac{aM_2(\eta)}{D} = \sum_{n=1,2,\dots}^{\infty} E_n \sin n\pi\eta \quad (2.22)$$

In contrast to doubly symmetric mode, the symmetric terms in Equation 2.10 and 2.11 should be deleted because of the simple support condition along the edge  $\eta = 0$  and  $\xi = 0$ . Enforcing the boundary condition of zero displacement and the equilibrium of moment along the edge  $\eta = l$ , the analytical function  $Y_m(\eta)$  in the doubly antisymmetric modes for  $\lambda^2 > (m\pi)^2$  may be written as,

$$Y_m(\eta) = E_m (\theta_{m11} \sinh \beta_m \eta + \theta_{m12} \sin \gamma_m \eta) \quad (2.23)$$

where,

$$\theta_{m11} = \frac{-1.0}{(\beta_m^2 + \gamma_m^2) \sinh \beta_m}, \text{ and } \theta_{m12} = \frac{1.0}{(\beta_m^2 + \gamma_m^2) \sin \gamma_m}$$

and for  $\lambda^2 < (m\pi)^2$ , the function  $Y_m(\eta)$  is given by

$$Y_m(\eta) = E_m (\theta_{m21} \sinh \beta_m \eta + \theta_{m22} \sinh \gamma_m \eta) \quad (2.24)$$

where,

$$\theta_{m21} = \frac{-1.0}{(\beta_m^2 - \gamma_m^2) \sinh \beta_m}, \text{ and } \theta_{m22} = \frac{1.0}{(\beta_m^2 - \gamma_m^2) \sinh \gamma_m}$$

where,  $\beta_m = \Phi \sqrt{\lambda^2 + (m\pi)^2}$  and  $\gamma_m = \Phi \sqrt{\lambda^2 - (m\pi)^2}$  or  $\Phi \sqrt{(m\pi)^2 - \lambda^2}$

Identically to the steps used in the doubly symmetric modes, the analytical function for the second building block,  $Y_n(\xi)$ , can be easily obtained from the first building block by interchange of coordinates. The aspect ratio must be replaced by its inverse and  $\lambda^2$  must be multiplied by  $\Phi^2$ . The analytical functions of the second building block are expressed as follows.

For  $\Phi^2\lambda^2 > (n\pi)^2$

$$Y_n(\xi) = E_n (\theta_{n11} \sinh \beta_n \xi + \theta_{n12} \sin \gamma_n \xi) \quad (2.25)$$

where,

$$\theta_{n11} = \frac{-1.0}{(\beta_n^2 + \gamma_n^2) \sinh \beta_n}, \text{ and } \theta_{n12} = \frac{1.0}{(\beta_n^2 + \gamma_n^2) \sin \gamma_n}$$

and for  $\Phi^2\lambda^2 < (n\pi)^2$ ,

$$Y_n(\xi) = E_n (\theta_{n21} \sinh \beta_n \xi + \theta_{n22} \sin \gamma_n \xi) \quad (2.26)$$

where,

$$\theta_{n21} = \frac{-1.0}{(\beta_n^2 - \gamma_n^2) \sinh \beta_n}, \text{ and } \theta_{n22} = \frac{1.0}{(\beta_n^2 - \gamma_n^2) \sin \gamma_n}$$

where,  $\beta_n = (1/\Phi) \sqrt{\lambda^2 \Phi^2 + (n\pi)^2}$ ,

and  $\gamma_n = (1/\Phi) \sqrt{\lambda^2 \Phi^2 - (n\pi)^2}$  or  $(1/\Phi) \sqrt{(n\pi)^2 - \lambda^2 \Phi^2}$

whichever is real.

### ***Symmetric-Antisymmetric Modes***

The building blocks used to analyse the symmetric-antisymmetric modes of fully clamped plates are illustrated in Figure 2.4. These building blocks have slip shear condition along the edge  $\eta = 0$  and the simple support condition along the edge  $\xi = 0$ . The edges  $\xi = 1$  and  $\eta = 1$  have simple support condition and are exposed to bending moment  $M_1(\xi)$  or  $M_2(\eta)$ .

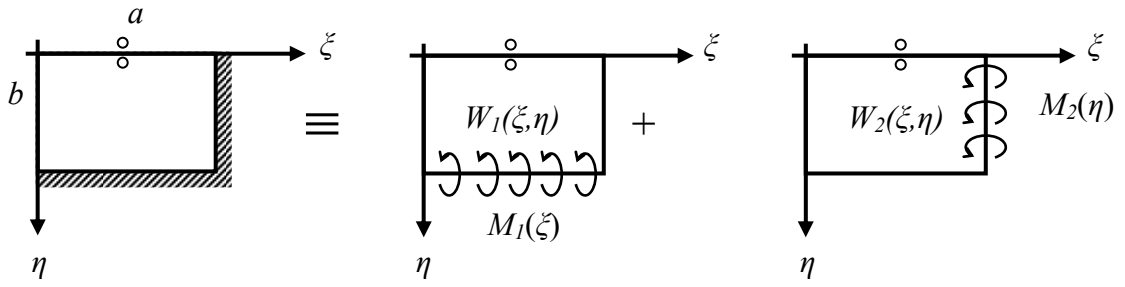


Figure 2.4 Building blocks used to analyse the symmetric- antisymmetric mode of fully clamped plates

The first and second building blocks have Lévy-type solutions, respectively, which can be written

$$W_1(\xi, \eta) = \sum_{m=1,2}^{\infty} Y_m(\eta) \sin m\pi\xi \quad (2.27)$$

and

$$W_2(\xi, \eta) = \sum_{n=1,3,5}^{\infty} Y_n(\xi) \cos \frac{n\pi\eta}{2} \quad (2.28)$$

Since the boundary conditions at the edges  $\eta = 0$  and  $\eta = 1$  of the first building block for the symmetric-antisymmetric modes are the same as those for the doubly symmetric modes, the analytical function  $Y_m(\eta)$  can be expressed in the same manner as Equation 2.15 and 2.16. However, the quantity  $m\pi/2$  in  $\beta_m$  and  $\gamma_m$  must be changed to  $m\pi$  and all positive integers can be taken for  $m$ , because the trigonometric function employed in Equation 2.7 is replaced with  $\sin(m\pi\xi)$ . It is written as follows.

For  $\lambda^2 > (m\pi)^2$

$$Y_m(\eta) = E_m (\theta_{m11} \cosh \beta_m \eta + \theta_{m12} \cos \gamma_m \eta) \quad (2.29)$$

where,

$$\theta_{m11} = \frac{-1.0}{(\beta_m^2 + \gamma_m^2) \cosh \beta_m}, \text{ and } \theta_{m12} = \frac{1.0}{(\beta_m^2 + \gamma_m^2) \cos \gamma_m}$$

and for  $\lambda^2 < (m\pi)^2$ ,

$$Y_m(\eta) = E_m (\theta_{m21} \cosh \beta_m \eta + \theta_{m22} \cosh \gamma_m \eta) \quad (2.30)$$

where,

$$\theta_{m21} = \frac{-1.0}{(\beta_m^2 - \gamma_m^2) \cosh \beta_m}, \text{ and } \theta_{m22} = \frac{1.0}{(\beta_m^2 - \gamma_m^2) \cosh \gamma_m}$$

with,  $\beta_m = \Phi\sqrt{\lambda^2 + (m\pi)^2}$

and  $\gamma_m = \Phi\sqrt{\lambda^2 - (m\pi)^2}$  or  $\Phi\sqrt{(m\pi)^2 - \lambda^2}$

whichever is real.

Similarly the second building block solution can be obtained from the previous mode families. The boundary conditions at the edges  $\xi = 0$  and  $\xi = 1$  are identical to those of the doubly antisymmetric modes. Thus, the analytical function  $Y_n(\xi)$  in Equation 2.28 would have the same form as Equation 2.25 and 2.26. However, the quantity  $n\pi$  in  $\beta_n$  and  $\gamma_n$  must be changed to  $n\pi/2$ . It is expressed as follows.

For  $\Phi^2\lambda^2 > (n\pi/2)^2$

$$Y_n(\xi) = E_n (\theta_{n11} \sinh \beta_n \xi + \theta_{n12} \sin \gamma_n \xi) \quad (2.31)$$

where,

$$\theta_{n11} = \frac{-1.0}{(\beta_n^2 + \gamma_n^2) \sinh \beta_n}, \text{ and } \theta_{n12} = \frac{1.0}{(\beta_n^2 + \gamma_n^2) \sin \gamma_n}$$

and for  $\Phi^2\lambda^2 < (n\pi/2)^2$ ,

$$Y_n(\xi) = E_n (\theta_{n21} \sinh \beta_n \xi + \theta_{n22} \sinh \gamma_n \xi) \quad (2.32)$$

where,

$$\theta_{n21} = \frac{-1.0}{(\beta_n^2 - \gamma_n^2) \sinh \beta_n}, \text{ and } \theta_{n22} = \frac{1.0}{(\beta_n^2 - \gamma_n^2) \sinh \gamma_n}$$

where,  $\beta_n = (1/\Phi)\sqrt{\lambda^2\Phi^2 + (n\pi/2)^2}$ ,

and  $\gamma_n = (1/\Phi)\sqrt{\lambda^2\Phi^2 - (n\pi/2)^2}$  or  $(1/\Phi)\sqrt{(n\pi/2)^2 - \lambda^2\Phi^2}$

whichever is real.

In order to generate the eigenvalue equation, the two building blocks are superimposed. The summation of contributions of each building block to the slope along the edges  $\xi = 1$  and  $\eta = 1$  should satisfy the boundary condition of zero net slope normal to the edges  $\xi = 1$  and  $\eta = 1$ . The net slope normal to these edges should be expanded in appropriate trigonometric series [2]. If utilising  $K_f$  terms in each of building blocks, one will obtain a set of  $2K_f$  homogenous algebraic equations relating moment coefficients  $E$ . Eigenvalues of the set of  $2K_f$  equations could be obtained by seeking the parameter  $\lambda^2$  which make the determinant of the eigenvalue matrix vanish.

### 2.1.2. Completely Free Plate

Similar to the case of the fully clamped plate, only quarter plate with dimension of  $a \times b$  is considered, and different family of modes are analysed separately.

#### *Doubly Symmetric Mode*

The building blocks of the completely free plate for the doubly symmetric modes are depicted in Figure 2.5. The origin of the quarter plate is taken on the centre of original plate, and bending moment is applied on the edges  $\zeta = l$  and  $\eta = l$ . A solution of the first block could also be expressed as Lévy-type, which is

$$W_1(\zeta, \eta) = \sum_{m=0,1}^{\infty} Y_m(\eta) \cos m\pi\zeta \quad (2.33)$$

Equation 2.33 satisfies the shear-slip condition at the edges  $\zeta = 0$  and  $\zeta = l$ .

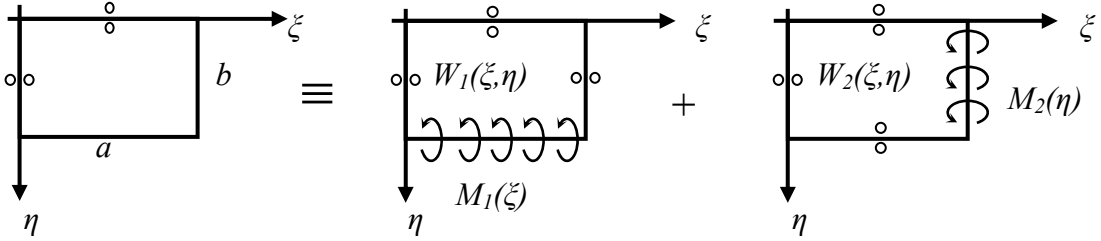


Figure 2.5 Building blocks used to analyse the fully symmetric mode of the completely free plate

Substituting Equation 2.33 into the governing differential equation, one will obtain the typical solutions of  $Y_m(\eta)$  as same as Equations 2.10 and 2.11 depending on  $\lambda^2$  is greater than or less than  $(m\pi)^2$ , where,

$$\beta_m = \Phi \sqrt{\lambda^2 + (m\pi)^2}$$

and

$$\gamma_m = \Phi \sqrt{\lambda^2 - (m\pi)^2} \text{ or } \Phi \sqrt{(m\pi)^2 - \lambda^2} .$$

Again, because the solution must be symmetric about the  $\xi$ -axis, two coefficients will be eliminated so that only symmetric terms in Equation 2.10 and 2.11 will remain. The other two coefficients are determined by enforcing the boundary condition of zero vertical edge reaction and the equilibrium of edge rotation along the edge  $\eta = l$ . The edge rotation should be expressed by the following Fourier expansion

$$\frac{\partial W_1(\xi, \eta)}{\partial \eta} = \sum_{m=0,1,\dots}^{\infty} E_m \cos m\pi\xi \quad (2.34)$$

Substituting Equation 2.10 and 2.11 without sine and hyperbolic sine terms into Equation 2.5 and setting its left right hand side equal to zero, furthermore, applying the relationship of Equation 2.34, then the analytical function  $Y_m(\eta)$  can be expressed in terms of the coefficients  $E_m$ , as follows.

For  $\lambda^2 > (m\pi)^2$

$$Y_m(\eta) = E_m (\theta_{m11} \cosh \beta_m \eta + \theta_{m12} \cos \gamma_m \eta) \quad (2.35)$$

where  $\theta_{m11} = 1/\{(\beta_m - ZZ1\gamma_m/ZZ2)\sinh \beta_m\}$

and  $\theta_{m12} = ZZ1/\{ZZ2(\beta_m - ZZ1\gamma_m/ZZ2)\sin \gamma_m\}$

with  $ZZ1 = -\beta_m \{\beta_m^2 - \nu^* \Phi^2(m\pi)^2\}$

and  $ZZ2 = \gamma_m \{\gamma_m^2 + \nu^* \Phi^2(m\pi)^2\}$

and, for  $\lambda^2 < (m\pi)^2$

$$Y_m(\eta) = E_m (\theta_{m21} \cosh \beta_m \eta + \theta_{m22} \cosh \gamma_m \eta) \quad (2.36)$$

where  $\theta_{m21} = 1/\{(\beta_m - ZZ1\gamma_m/ZZ2)\sinh \beta_m\}$

and  $\theta_{m22} = ZZ1/\{ZZ2(\beta_m + ZZ1\gamma_m/ZZ2)\sinh \gamma_m\}$

with  $ZZ1 = -\beta_m \{\beta_m^2 - \nu^* \Phi^2(m\pi)^2\}$

and  $ZZ2 = \gamma_m \{\gamma_m^2 - \nu^* \Phi^2(m\pi)^2\}$

Next, the analytical function  $Y_n(\xi)$  for the second building block can be obtained from the first building block by interchange of coordinate due to symmetry as explained in the fully clamped case. Once again the aspect ratio must be replaced by its inverse and  $\lambda^2$  must be multiplied by  $\Phi^2$ . The displacement function of the second building block is

$$W_2(\xi, \eta) = \sum_{n=0,1,2}^{\infty} Y_n(\xi) \cos n\pi\eta \quad (2.37)$$

The analytical functions are expressed as follows.

For  $\Phi^2 \lambda^2 > (n\pi)^2$

$$Y_n(\xi) = E_n (\theta_{n11} \cosh \beta_n \xi + \theta_{n12} \cos \gamma_n \xi) \quad (2.38)$$

where  $\theta_{n11} = 1 / \{(\beta_n - ZZ1 \gamma_n / ZZ2) \sinh \beta_n\}$

and  $\theta_{n12} = ZZ1 / \{ZZ2(\beta_n - ZZ1 \gamma_n / ZZ2) \sin \gamma_n\}$

with  $ZZ1 = -\beta_n \{\beta_n^2 - \nu^* / \Phi^2 (n\pi)^2\}$

and  $ZZ2 = \gamma_n \{\gamma_n^2 + \nu^* / \Phi^2 (n\pi)^2\}$

and, for  $\Phi^2 \lambda^2 < (n\pi)^2$

$$Y_n(\xi) = E_n (\theta_{n21} \cosh \beta_n \xi + \theta_{n22} \cosh \gamma_n \xi) \quad (2.39)$$

where  $\theta_{n21} = 1 / \{(\beta_n - ZZ1 \gamma_n / ZZ2) \sinh \beta_n\}$

and  $\theta_{n22} = ZZ1 / \{ZZ2(\beta_n + ZZ1 \gamma_n / ZZ2) \sinh \gamma_n\}$

with  $ZZ1 = -\beta_n \{\beta_n^2 - \nu^* / \Phi^2 (n\pi)^2\}$

and  $ZZ2 = \gamma_n \{\gamma_n^2 - \nu^* / \Phi^2 (n\pi)^2\}$

with

$$\beta_n = 1/\Phi \sqrt{\Phi^2 \lambda^2 + (n\pi)^2}$$

and

$$\gamma_n = 1/\Phi \sqrt{\Phi^2 \lambda^2 - (n\pi)^2} \text{ or } 1/\Phi \sqrt{(n\pi)^2 - \Phi^2 \lambda^2}$$

whichever is real.

### ***Doubly Antisymmetric Mode***

The steps to obtain the functions  $Y_m(\eta)$  and  $Y_n(\xi)$  are identical to those explained in the doubly antisymmetric mode of fully clamped plate problem. For fully antisymmetric modes, slip-shear conditions must be replaced by simple support conditions along the  $\xi$  and  $\eta$  axes as shown in Figure 2.6. In such case, the displacement functions  $W_1$  and  $W_2$  will be expressed as

$$W_1(\xi, \eta) = \sum_{m=1,3,5}^{\infty} Y_m(\eta) \sin \frac{m\pi\xi}{2} \quad (2.40)$$

and

$$W_2(\xi, \eta) = \sum_{n=1,3,5}^{\infty} Y_n(\xi) \sin \frac{n\pi\eta}{2} \quad (2.41)$$

respectively. The trigonometric function employed in Equation 2.33 or 2.37 is replaced by  $\sin(m\pi\xi/2)$  or  $\sin(n\pi\eta/2)$ .

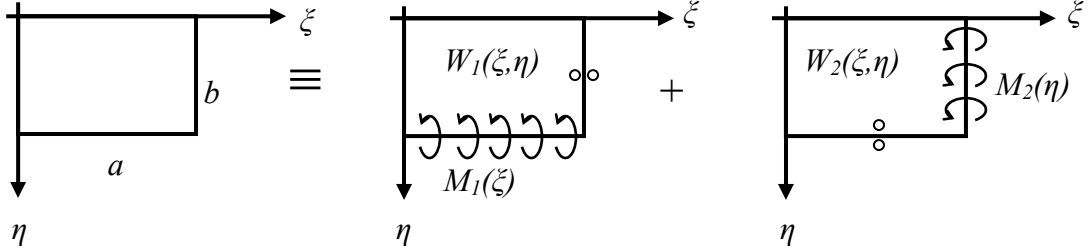


Figure 2.6 Building blocks used to analyse the fully antisymmetric mode of the completely free plate

These functions  $Y_m(\eta)$  and  $Y_n(\xi)$  will take the same form as Equation 2.10 and 2.11 depending whether or not  $\lambda^2$  is greater than  $(m\pi/2)^2$  or  $(n\pi/2)^2$ . However, the symmetric terms in Equation 2.10 and 2.11 should be deleted because of the simple support condition along the edge  $\eta = 0$  and  $\xi = 0$ . Applying the boundary conditions of zero vertical edge reaction and the equilibrium of edge rotation along the edge  $\eta = l$ , the functions  $Y_m(\eta)$  written as follows

For  $\lambda^2 > (m\pi/2)^2$

$$Y_m(\eta) = E_m (\theta_{m11} \sinh \beta_m \eta + \theta_{m12} \sin \gamma_m \eta) \quad (2.42)$$

where  $\theta_{m11} = 1 / \{ (\beta_m + ZZ1\gamma_m / ZZ2) \cosh \beta_m \}$

and  $\theta_{m12} = ZZ1 / \{ ZZ2(\beta_m + ZZ1\gamma_m / ZZ2) \cos \gamma_m \}$

with  $ZZ1 = \beta_m \{ \beta_m^2 - \nu^* \Phi^2 (m\pi/2)^2 \}$

and  $ZZ2 = \gamma_m \{ \gamma_m^2 + \nu^* \Phi^2 (m\pi/2)^2 \}$

and, for  $\lambda^2 < (m\pi/2)^2$

$$Y_m(\eta) = E_m (\theta_{m21} \sinh \beta_m \eta + \theta_{m22} \sinh \gamma_m \eta) \quad (2.43)$$

where  $\theta_{m21} = 1 / \{ (\beta_m + ZZ1\gamma_m / ZZ2) \cosh \beta_m \}$

and  $\theta_{m22} = ZZ1 / \{ ZZ2(\beta_m + ZZ1\gamma_m / ZZ2) \cosh \gamma_m \}$

with  $ZZ1 = -\beta_m \{ \beta_m^2 - \nu^* \Phi^2 (m\pi/2)^2 \}$

and  $ZZ2 = \gamma_m \{ \gamma_m^2 - \nu^* \Phi^2 (m\pi/2)^2 \}$

with

$$\beta_m = \Phi \sqrt{\lambda^2 + (m\pi/2)^2}$$

and

$$\gamma_m = \Phi \sqrt{\lambda^2 - (m\pi/2)^2} \text{ or } \Phi \sqrt{(m\pi/2)^2 - \lambda^2}$$

whichever is real.

The function  $Y_n(\xi)$  is obtained in the same manner of the doubly symmetric mode. The aspect ratio is replaced by its inverse and  $\lambda^2$  must be multiplied by  $\Phi^2$  and for  $\Phi^2 \lambda^2 > (n\pi/2)$  the function  $Y_n(\xi)$  is,

$$Y_n(\xi) = E_n (\theta_{n11} \sinh \beta_n \xi + \theta_{n12} \sin \gamma_n \xi) \quad (2.44)$$

where  $\theta_{n11} = 1/\{(\beta_n + ZZ1\gamma_n/ZZ2)\cosh \beta_n\}$

and  $\theta_{n12} = ZZ1/\{ZZ2(\beta_n + ZZ1\gamma_n/ZZ2)\cos \gamma_n\}$

with  $ZZ1 = \beta_n \{\beta_n^2 - \nu^*/\Phi^2 (n\pi/2)^2\}$

and  $ZZ2 = \gamma_n \{\gamma_n^2 + \nu^*/\Phi^2 (n\pi/2)^2\}$

and, for  $\Phi^2 \lambda^2 < (n\pi/2)^2$

$$Y_n(\xi) = E_n (\theta_{n21} \sinh \beta_n \xi + \theta_{n22} \sinh \gamma_n \xi) \quad (2.45)$$

where  $\theta_{n21} = 1/\{(\beta_n + ZZ1\gamma_n/ZZ2)\cosh \beta_n\}$

and  $\theta_{n22} = ZZ1/\{ZZ2(\beta_n + ZZ1\gamma_n/ZZ2)\cosh \gamma_n\}$

with  $ZZ1 = -\beta_n \{\beta_n^2 - \nu^*/\Phi^2 (n\pi/2)^2\}$

and  $ZZ2 = \gamma_n \{\gamma_n^2 - \nu^*/\Phi^2 (n\pi/2)^2\}$

with

$$\beta_n = 1/\Phi \sqrt{\Phi^2 \lambda^2 + (n\pi/2)^2}$$

and

$$\gamma_n = 1/\Phi \sqrt{\Phi^2 \lambda^2 - (n\pi/2)^2} \text{ or } 1/\Phi \sqrt{(n\pi/2)^2 - \Phi^2 \lambda^2}$$

whichever is real.

### ***Symmetric-Antisymmetric Mode***

The building blocks used to analyse the symmetric-antisymmetric modes of the completely free plates are illustrated in Figure 2.7. These building blocks have slip shear condition along the edge  $\eta = 0$  and the simple support condition along

the edge  $\zeta = 0$ . The edges  $\zeta = 1$  and  $\eta = 1$  have shear slip condition and are exposed to bending moment  $M_1(\zeta)$  or  $M_2(\eta)$ .

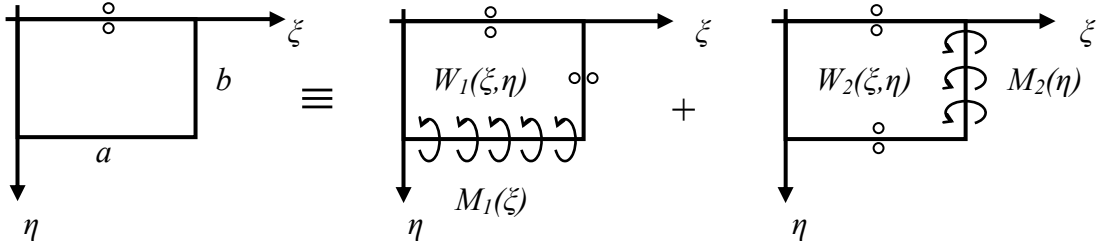


Figure 2.7 Building blocks used to analyse the symmetric-antisymmetric mode of the completely free plate

The first and second building blocks have Lévy-type solutions, respectively, which can be written

$$W_1(\xi, \eta) = \sum_{m=1,3,5}^{\infty} Y_m(\eta) \sin \frac{m\pi\xi}{2} \quad (2.46)$$

and

$$W_2(\xi, \eta) = \sum_{n=0,1,2}^{\infty} Y_n(\xi) \cos n\pi\eta \quad (2.47)$$

Since the boundary conditions at the edges  $\eta = 0$  and  $\eta = 1$  of the first building block for the symmetric-antisymmetric modes are the same as those for the doubly symmetric modes, the analytical function  $Y_m(\eta)$  can be expressed in the same manner as Equation 2.35 and 2.36. However, the quantity  $m\pi$  in  $\beta_m$  and  $\gamma_m$  must be changed to  $m\pi/2$ , because the trigonometric function employed in Equation 2.33 is replaced with  $\sin(m\pi\xi/2)$ . It is written as follows.

For  $\lambda^2 > (m\pi/2)^2$

$$Y_m(\eta) = E_m (\theta_{m11} \cosh \beta_m \eta + \theta_{m12} \cos \gamma_m \eta) \quad (2.48)$$

where  $\theta_{m11} = 1 / \{ (\beta_m - ZZ1\gamma_m / ZZ2) \sinh \beta_m \}$

and  $\theta_{m12} = ZZ1 / \{ ZZ2(\beta_m - ZZ1\gamma_m / ZZ2) \sin \gamma_m \}$

with  $ZZ1 = -\beta_m \{ \beta_m^2 - \nu^* \Phi^2(m\pi/2)^2 \}$

and  $ZZ2 = \gamma_m \{ \gamma_m^2 + \nu^* \Phi^2(m\pi/2)^2 \}$

and, for  $\lambda^2 < (m\pi/2)$

$$Y_m(\eta) = E_m(\theta_{m21} \cosh \beta_m \eta + \theta_{m22} \cosh \gamma_m \eta) \quad (2.49)$$

where  $\theta_{m21} = 1/\{(\beta_m - ZZ1\gamma_m/ZZ2)\sinh \beta_m\}$

and  $\theta_{m22} = ZZ1/\{ZZ2(\beta_m + ZZ1\gamma_m/ZZ2)\sinh \gamma_m\}$

with  $ZZ1 = -\beta_m \{\beta_m^2 - \nu^* \Phi^2 (m\pi/2)^2\}$

and  $ZZ2 = \gamma_m \{\gamma_m^2 - \nu^* \Phi^2 (m\pi/2)^2\}$

with,

$$\beta_m = \Phi \sqrt{\lambda^2 + (m\pi/2)^2}$$

and

$$\gamma_m = \Phi \sqrt{\lambda^2 - (m\pi/2)^2} \text{ or } \Phi \sqrt{(m\pi/2)^2 - \lambda^2}$$

whichever is real.

Similarly the second building block solution can be obtained from the previous mode families. The boundary conditions at the edges  $\zeta = 0$  and  $\zeta = 1$  are identical to those of the doubly antisymmetric modes. Thus, the analytical function  $Y_n(\zeta)$  in Equation 2.47 would have the same form as Equation 2.44 and 2.45. However, the quantity  $n\pi/2$  in  $\beta_n$  and  $\gamma_n$  must be changed to  $n\pi$ . It is expressed as follows.

For  $\Phi^2 \lambda^2 > (n\pi)^2$

$$Y_n(\xi) = E_n(\theta_{n11} \sinh \beta_n \xi + \theta_{n12} \sin \gamma_n \xi) \quad (2.50)$$

where  $\theta_{n11} = 1/\{(\beta_n + ZZ1\gamma_n/ZZ2)\cosh \beta_n\}$

and  $\theta_{n12} = ZZ1/\{ZZ2(\beta_n + ZZ1\gamma_n/ZZ2)\cos \gamma_n\}$

with  $ZZ1 = \beta_n \{\beta_n^2 - \nu^*/\Phi^2 (n\pi)^2\}$

and  $ZZ2 = \gamma_n \{\gamma_n^2 + \nu^*/\Phi^2 (n\pi)^2\}$

and, for  $\Phi^2 \lambda^2 < (n\pi)^2$

$$Y_n(\xi) = E_n(\theta_{n21} \sinh \beta_n \xi + \theta_{n22} \sinh \gamma_n \xi) \quad (2.51)$$

where  $\theta_{n21} = 1/\{(\beta_n + ZZ1\gamma_n/ZZ2)\cosh \beta_n\}$

and  $\theta_{n22} = ZZ1/\{ZZ2(\beta_n + ZZ1\gamma_n/ZZ2)\cosh \gamma_n\}$

with  $ZZ1 = -\beta_n \{\beta_n^2 - \nu^*/\Phi^2 (n\pi)^2\}$

and  $ZZ2 = \gamma_n \{\gamma_n^2 - \nu^*/\Phi^2 (n\pi)^2\}$

with

$$\beta_n = 1/\Phi \sqrt{\Phi^2 \lambda^2 + (n\pi)^2}$$

and

$$\gamma_n = 1/\Phi \sqrt{\Phi^2 \lambda^2 - (n\pi)^2} \text{ or } 1/\Phi \sqrt{(n\pi)^2 - \Phi^2 \lambda^2} .$$

whichever is real.

The eigenvalue equation is generated in the same manner as for the fully clamped plate. The summation of contributions of each building block to the moment along the edges  $\zeta = l$  and  $\eta = l$  should satisfy the boundary condition of zero net moment along the edges  $\zeta = l$  and  $\eta = l$ . The eigenvalues are obtained by searching for the parameter  $\lambda^2$  which cause the determinant of the eigenvalue matrix to vanish.

## 2.2. The Finite Difference Method

The finite difference method is explained in detail by Smith [6]. For the sake of completeness the essential derivations are presented here. When there is a function  $U$ , and the function and its derivatives are finite and continuous function of only  $x$ , then it can be expanded as follows using Taylor's theorem,

$$U(x_1 + h) = U(x_1) + hU'(x_1) + \frac{1}{2}h^2U''(x_1) + \frac{1}{6}h^3U'''(x_1) + \dots \quad (2.52)$$

and

$$U(x_1 - h) = U(x_1) - hU'(x_1) + \frac{1}{2}h^2U''(x_1) - \frac{1}{6}h^3U'''(x_1) + \dots \quad (2.53)$$

Summation of the Equations 2.52 and 2.53 gives

$$U(x_1 + h) + U(x_1 - h) = U(x_1) + h^2U''(x_1) + O(h^4) \quad (2.54)$$

where  $O(h^4)$  denotes terms that contains fourth and higher powers of  $h$ . If it is assumed that these terms can be ignored because they are much smaller than lower powers of  $h$ , then

$$U''(x_1) = \left( \frac{d^2U}{dx^2} \right)_{x=x_1} \cong \frac{1}{h^2} \{U(x_1 + h) - U(x_1) + U(x_1 - h)\} \quad (2.55)$$

Subtracting Equation 2.53 from Equation 2.52 and neglect terms containing third and higher powers of  $h$ , one obtains,

$$U'(x_1) = \left( \frac{dU}{dx} \right)_{x=x_1} \cong \frac{1}{2h} \{U(x_1 + h) - U(x_1 - h)\} \quad (2.56)$$

Equation 2.56 is a central-difference approximation of the first derivative of function  $U$  at  $x = x_1$ .

In this thesis, the plate to be analysed is meshed as shown in Figure 2.8 (a) and Equation 2.1 is approximated in the finite difference form with central-difference approximation, in term of the nodal displacements. The molecular FD equation at node  $(i,j)$  depends on the values of displacement of this and adjacent nodes shown in Figure 2.8 (b). The FD molecules used in this thesis are based on the literature [7]. The basic finite difference operators are given below.

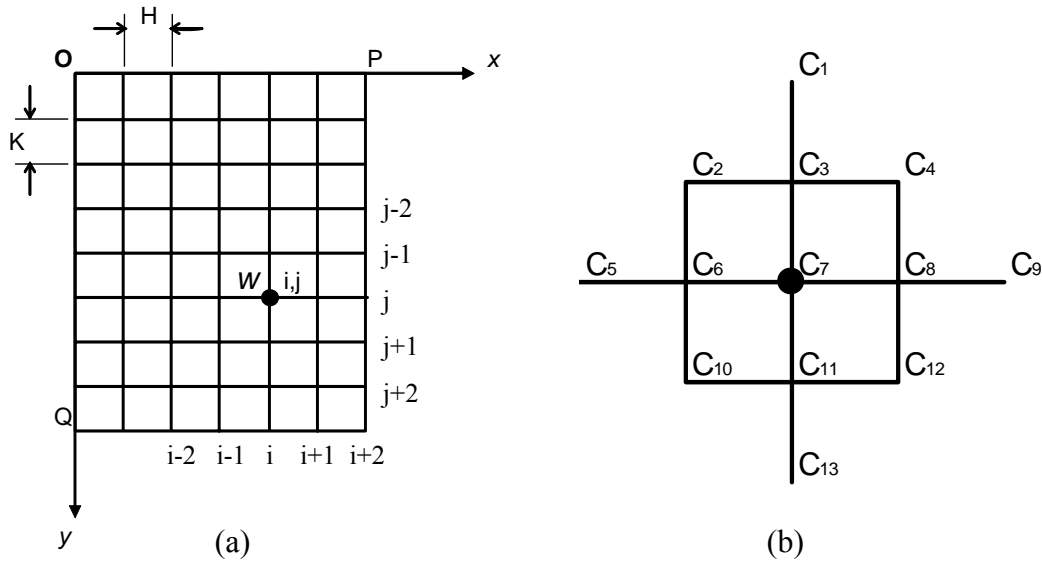


Figure 2.8 The F.D. Scheme for a plate (a) the mesh and a typical node and (b) the F. D. molecular formula

$$\left( \frac{\partial w}{\partial x} \right)_{i,j} = \frac{w_{i+1,j} - w_{i-1,j}}{2H}, \quad \left( \frac{\partial w}{\partial y} \right)_{i,j} = \frac{w_{i,j+1} - w_{i,j-1}}{2K} \quad (2.57, 58)$$

$$\left( \frac{\partial^2 w}{\partial x^2} \right)_{i,j} = \frac{w_{i-1,j} - 2w_{i,j} + w_{i+1,j}}{H^2}, \quad \left( \frac{\partial^2 w}{\partial y^2} \right)_{i,j} = \frac{w_{i,j-1} - 2w_{i,j} + w_{i,j+1}}{K^2} \quad (2.59, 60)$$

$$\left(\frac{\partial^2 w}{\partial x \partial y}\right)_{i,j} = \frac{w_{i-1,j-1} - w_{i+1,j-1} - w_{i-1,j+1} + w_{i+1,j+1}}{2HK} \quad (2.61)$$

$$\left(\frac{\partial^3 w}{\partial x^3}\right)_{i,j} = \frac{-w_{i-2,j} + 2w_{i-1,j} - 2w_{i+1,j} + w_{i+2,j}}{2H^3} \quad (2.62)$$

$$\left(\frac{\partial^3 w}{\partial x^2 \partial y}\right)_{i,j} = \frac{w_{i-1,j+1} - 2w_{i,j+1} + w_{i+1,j+1} - (w_{i-1,j-1} - 2w_{i,j-1} + w_{i+1,j-1})}{2H^2 K} \quad (2.63)$$

$$\left(\frac{\partial^3 w}{\partial y^3}\right)_{i,j} = \frac{-w_{i,j-2} + 2w_{i,j-1} - 2w_{i,j+1} + w_{i,j+2}}{2K^3} \quad (2.64)$$

$$\left(\frac{\partial^3 w}{\partial x \partial y^2}\right)_{i,j} = \frac{w_{i+1,j-1} - 2w_{i+1,j} + w_{i+1,j+1} - (w_{i-1,j-1} - 2w_{i-1,j} + w_{i-1,j+1})}{2HK^2} \quad (2.65)$$

$$\left(\frac{\partial^4 w}{\partial x^4}\right)_{i,j} = \frac{w_{i-2,j} - 4w_{i-1,j} + 6w_{i,j} - 4w_{i+1,j} + w_{i+2,j}}{H^4} \quad (2.66)$$

$$\left(\frac{\partial^4 w}{\partial y^4}\right)_{i,j} = \frac{w_{i,j-2} - 4w_{i,j-1} + 6w_{i,j} - 4w_{i,j+1} + w_{i,j+2}}{K^2} \quad (2.67)$$

$$\left(\frac{\partial^4 w}{\partial x^2 \partial y^2}\right)_{i,j} = \frac{w_{i-1,j-1} - 2w_{i,j-1} + w_{i+1,j-1} - 2(w_{i-1,j} - 2w_{i,j} + w_{i+1,j}) + w_{i-1,j+1} - 2w_{i,j+1} + w_{i+1,j+1}}{H^2 K^2} \quad (2.68)$$

The FD form of Equation 2.1 is,

$$\sum_{k=1}^{13} C_k w_k^* = 0 \quad (2.69)$$

where,

$$\begin{aligned} w_1^* &= w(i, j-2), & w_2^* &= w(i-1, j-1), & w_3^* &= w(i, j-1), \\ w_4^* &= w(i+1, j-1), & w_5^* &= w(i-2, j), & w_6^* &= w(i-1, j), & w_7^* &= w(i, j), \\ w_8^* &= w(i+1, j), & w_9^* &= w(i+2, j), & w_{10}^* &= w(i-1, j+1), \\ w_{11}^* &= w(i, j+1), & w_{12}^* &= w(i+1, j+1), & w_{13}^* &= w(i, j+2) \end{aligned} \quad (2.70)$$

$$C_1 = C_{13} = \frac{1}{K^4}, \quad C_5 = C_9 = \frac{1}{H^4} \quad (2.71, 72)$$

$$C_2 = C_{12} = \frac{2}{H^2 K^2}, \quad C_4 = C_{10} = \frac{2}{H^2 K^2} \quad (2.73, 74)$$

$$C_3 = C_{11} = -4\left(\frac{1}{K^4} + \frac{1}{H^2K^2}\right), \quad C_6 = C_8 = -4\left(\frac{1}{H^4} + \frac{1}{H^2K^2}\right) \quad (2.75, 76)$$

$$C7 = \left(\frac{6}{H^4} + \frac{6}{K^4} + \frac{8}{H^2K^2}\right) - \frac{m\omega^2}{D} \quad (2.77)$$

### 2.2.1. Fully Clamped plate

The distribution of nodes which F.D. equation applied at on an edge of fully clamped plate is shown in Figure 2.9, where  $w_1^*$  to  $w_{13}^*$  are the deflections of the nodes. The projected deflections outside of the plate need to be expressed in term of the deflections at the internal nodes by using the boundary conditions. The boundary conditions of a fully clamped plate, which are zero displacement and zero slope at the edges, are expressed by the following equations,

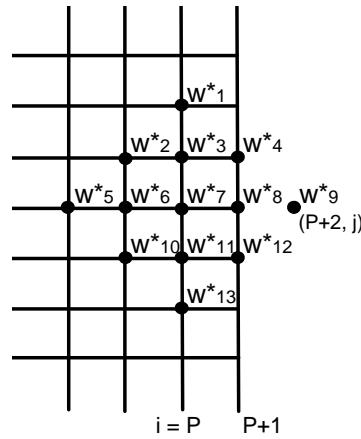


Figure 2.9 The node distribution at the edge of a fully clamped plate.

at  $x = 0$  or  $a$  ( $i = 0$  or  $P+1$ ),

$$w = 0 \quad (2.78a)$$

$$\left(\frac{\partial w}{\partial x}\right) = 0 \quad (2.78b)$$

at  $y = 0$  or  $b$  ( $j = 0$  or  $Q+1$ ),

$$w = 0 \quad (2.79a)$$

$$\left(\frac{\partial w}{\partial y}\right) = 0 \quad (2.79b)$$

## 2.2.2. Completely Free Plate

Figure 2.10 (a) and (b) show the distribution of nodes which F.D. equation applied at an edge and at a corner of the completely free plate respectively. Once again the projected deflections outside of the plate need to be expressed in term of the deflections at the internal nodes by using the boundary conditions.

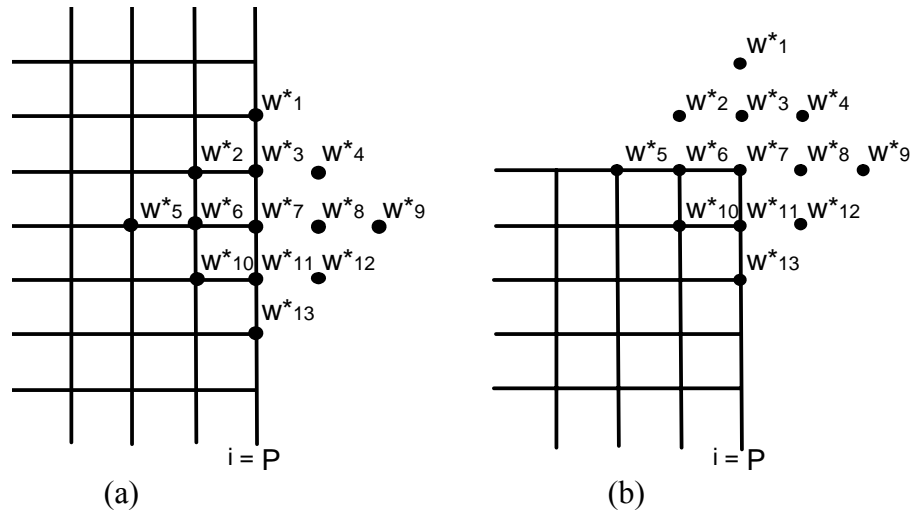


Figure 2.10 The node distribution for a completely free plate: (a) at the edge; (b) at the corner.

The boundary conditions of a free edge are given in Leissa's monograph [1]. Bending moment and vertical edge reaction at a free edge are zero. Those boundary conditions at the edges are expressed as,

at  $x = 0$  or a ( $i = I$  or  $P$ ),

$$\left(\frac{\partial^2 w}{\partial x^2}\right) + \nu \left(\frac{\partial^2 w}{\partial y^2}\right) = 0 \quad (2.80a)$$

$$\left(\frac{\partial^3 w}{\partial x^3}\right) + \nu^* \left(\frac{\partial^3 w}{\partial x \partial y^2}\right) = 0 \quad (2.80b)$$

at  $y = 0$  or b ( $j = I$  or  $Q$ ),

$$\left(\frac{\partial^2 w}{\partial y^2}\right) + \nu \left(\frac{\partial^2 w}{\partial x^2}\right) = 0 \quad (2.81a)$$

$$\left(\frac{\partial^3 w}{\partial y^3}\right) + \nu^* \left(\frac{\partial^3 w}{\partial x^2 \partial y}\right) = 0 \quad (2.81b)$$

The above boundary conditions are not enough to cover all nodes outside of the plate at the corners. The following boundary condition at the corners [1], is also needed.

$$\left( \frac{\partial^2 w}{\partial x \partial y} \right) = 0 \quad (\text{at the corners}) \quad (2.82)$$

# **Chapter III**

## **Numerical Results**

## 3. NUMERICAL RESULTS

The numerical results obtained using the superposition method and the finite difference method (FDM) are presented in this chapter. The natural frequencies of fully clamped plates and completely free plates are given in the dimensionless form,  $\lambda^2 = \omega a^2 \sqrt{\rho/D}$ , which will be referred to as the eigenvalue. The eigenvalue is importantly related to plate aspect ratio ( $\Phi = b/a$ ) rather than the dimensions of plate. All eigenvalues were calculated by using the software Matlab in default double precision.

### 3.1. *The Superposition Method*

The eigenvalues of fully clamped plates and completely free plates obtained using the superposition method are presented in this section. To make comparison of results between the superposition method and the FDM easier, the eigenvalues obtained by the superposition method are multiplied by a factor of four because the frequency parameters for the plates used in the superposition method is based on quarter size of original plate dimensions, while in the FDM analysis the non-dimensionalisation was done with respect to the full size of plate. This was done to facilitate comparison with published results.

#### 3.1.1. Fully Clamped Plate

Table 3.1 shows the first 12 eigenvalues of fully clamped plates with aspect ratios 1.0 to 3.0 obtained by the superposition method. The two letters adjacent to the values express type of modal shapes. SS, AA, SA and AS mean that the mode is symmetric about both the  $x$  and  $y$  axes, antisymmetric about both axes, symmetric about the  $x$ -axis and antisymmetric about the  $y$ -axis, and antisymmetric about the  $x$ -axis and symmetric about the  $y$ -axis respectively. The eigenvalues in

different family of modes were calculated separately. Because of symmetry in the boundary conditions, the eigenvalues for the SS and AA modes need to be calculated for only aspect ratios  $\Phi$  of one or greater. The eigenvalues for the SA modes, the aspect ratio varies from 1/3 to three due to lack of symmetry in the boundary conditions. The eigenvalues for SA mode for aspect ratio of 1/3 through to one would be the same as those for AS modes of the plates with aspect ratio of three through to one.

The eigenvalues presented here were calculated by utilising 15 terms, i.e. effective matrix size of  $60 \times 60$ , which is adequate for convergence to four significant places. It will be proved in the following convergence tests.

Table 3.1 The eigenvalues of fully clamped plates obtained by the superposition method ( $\lambda^2 = \omega a^2 \sqrt{\rho/D}$ ).

Mode	$\Phi = b/a$					
	1		1.25		1.5	
1	35.99	SS	29.89	SS	27.01	SS
2	73.39		52.51	AS	41.70	AS
3	73.39	SA or AS	68.51	SA	66.13	SA
4	108.2	AA	89.25	SS	66.52	SS
5	131.6	SS	89.35	AA	79.81	AA
6	132.2	SS	124.3	SA	100.8	AS
7	165.0		127.5	SS	103.1	SA
8	165.0	SA or AS	139.2	AS	125.3	SS
9	210.5		147.5	AS	136.1	AA
10	210.5	SA or AS	173.0	AA	138.6	AS
11	220.0	SS	181.3	SS	144.2	SS
12	242.2	AA	202.1	SS	161.2	SS

Mode	$\Phi = b/a$					
	2		2.5		3	
1	24.58	SS	23.64	SS	23.20	SS
2	31.83	AS	27.81	AS	25.86	AS
3	44.77	SS	35.42	SS	30.74	SS
4	63.33	AS	46.67	AS	38.09	AS
5	63.98	SA	61.49	SS	47.97	SS
6	71.08	AA	63.08	SA	60.30	AS
7	83.27	SA	67.39	AA	62.62	SA
8	87.25	SS	74.78	SA	65.51	AA
9	100.8	AA	79.76	AS	70.44	SA
10	116.4	AS	85.43	AA	75.04	SS
11	123.2	SS	99.46	SA	77.53	AA
12	123.7	SA	101.4	SS	86.90	SA

### Convergence test

A number of convergence tests were carried out for a range of aspect ratios and modes. The results are shown as follows. From the tests, it can be seen that the rate of convergence for the superposition method is rapid, and all of them converge from below.

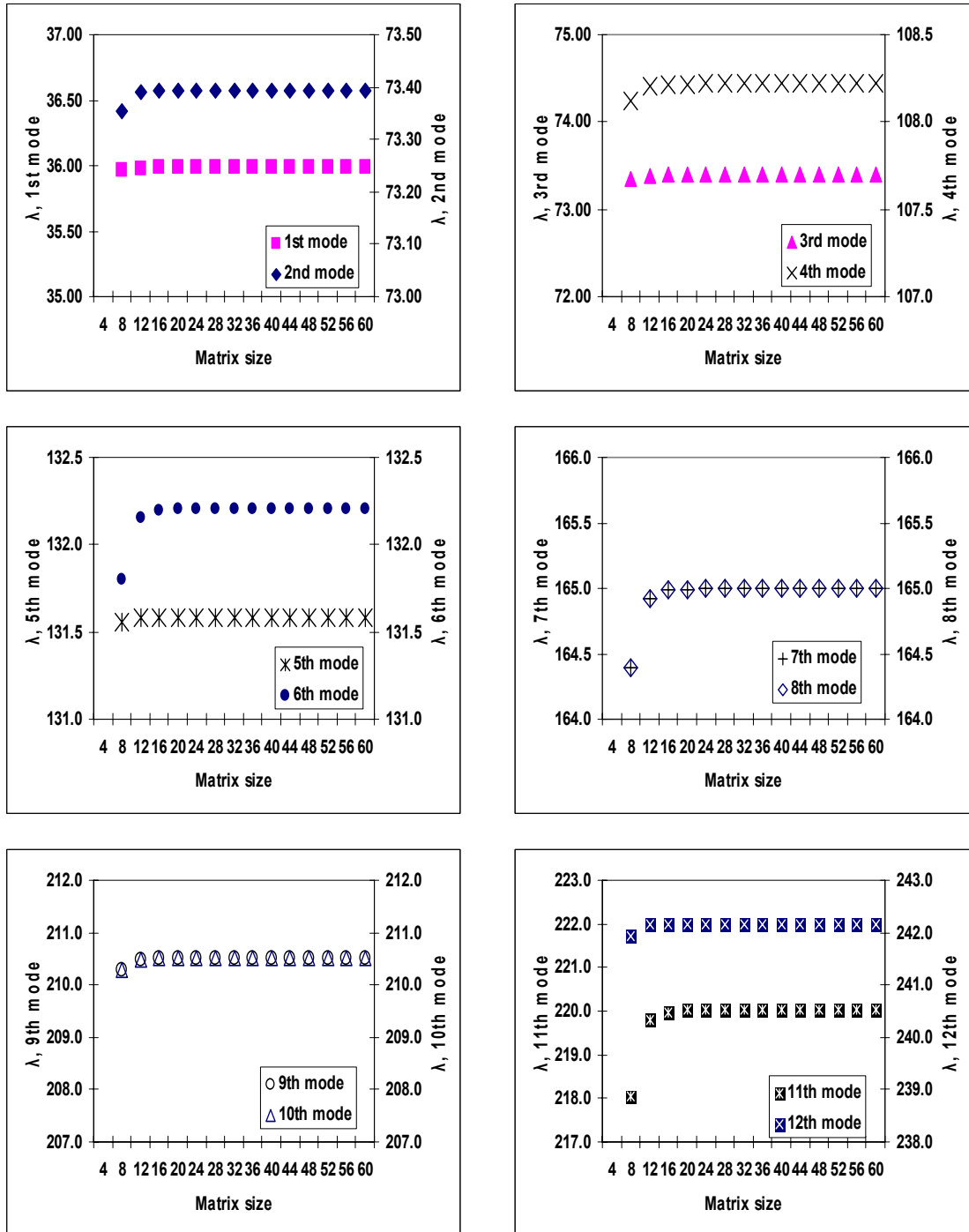


Figure 3.1 Convergence test for the eigenvalues of fully clamped rectangular plate computed by the superposition method ( $\Phi = 1.0$ )

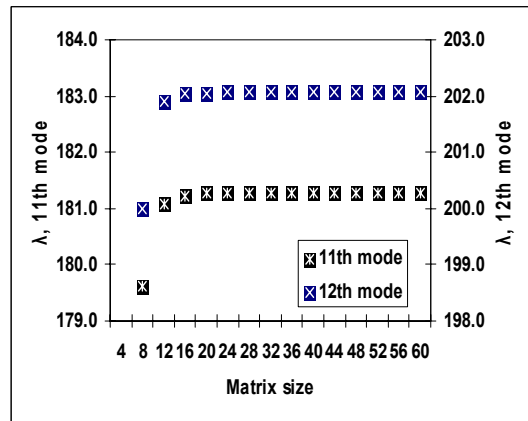
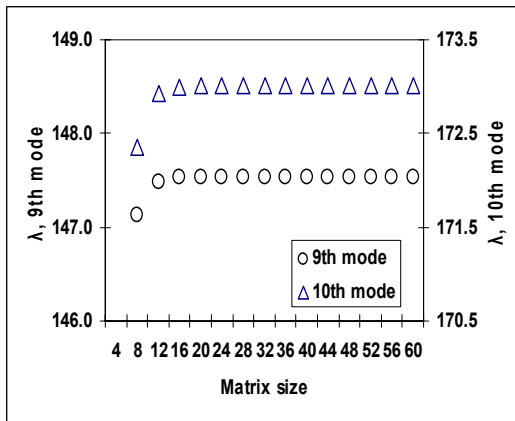
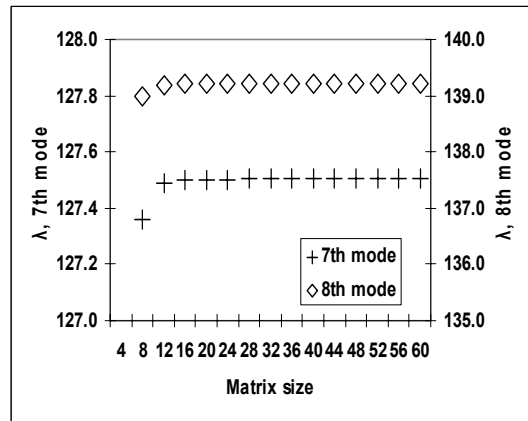
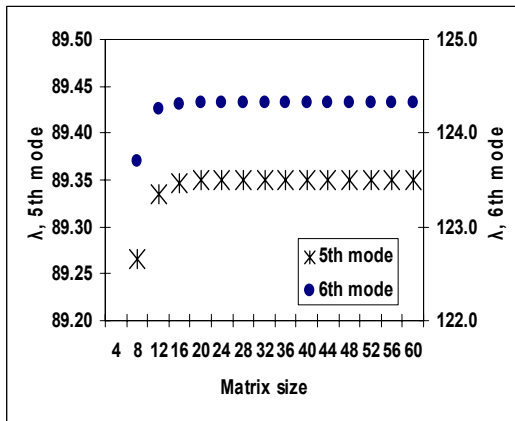
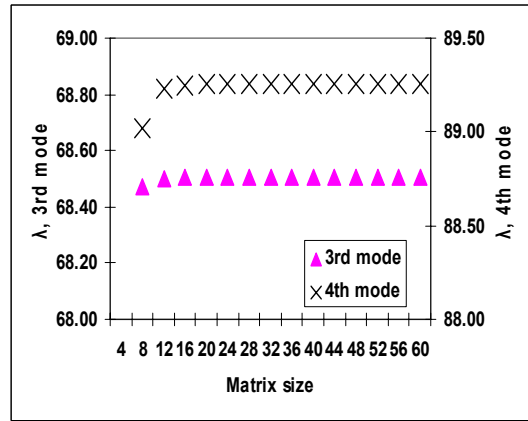
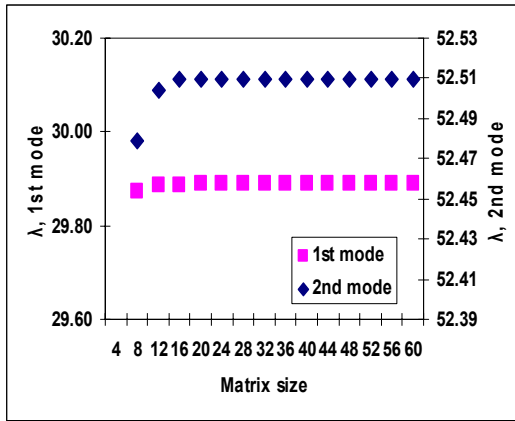


Figure 3.2 Convergence test for the eigenvalues of fully clamped rectangular plate computed by the superposition method ( $\Phi = 1.25$ )

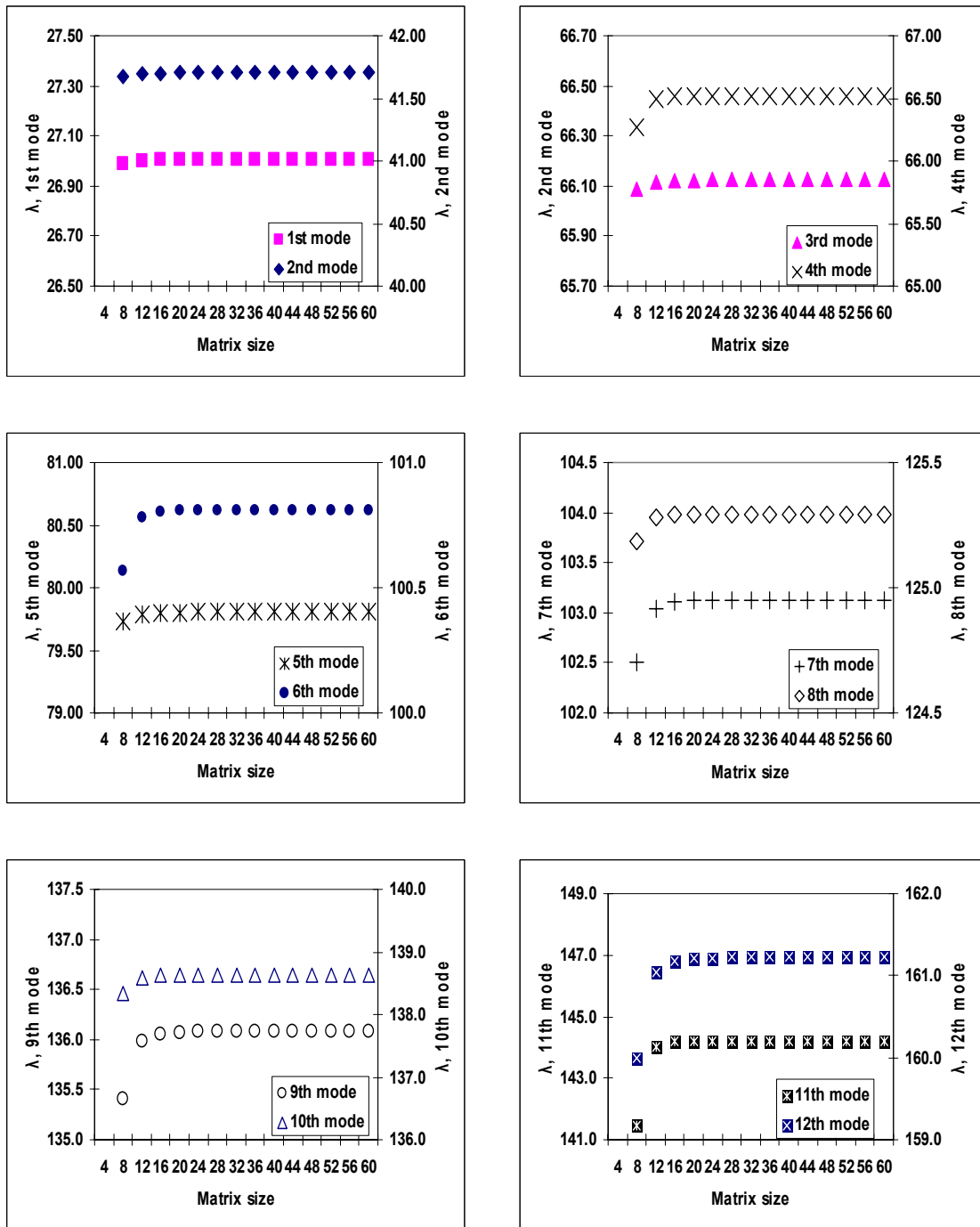


Figure 3.3 Convergence test for the eigenvalues of fully clamped rectangular plate computed by the superposition method ( $\Phi = 1.5$ )

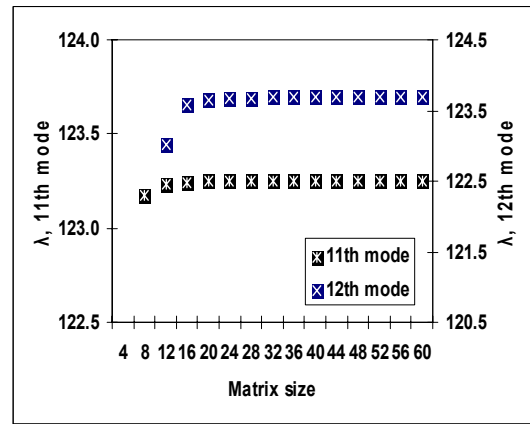
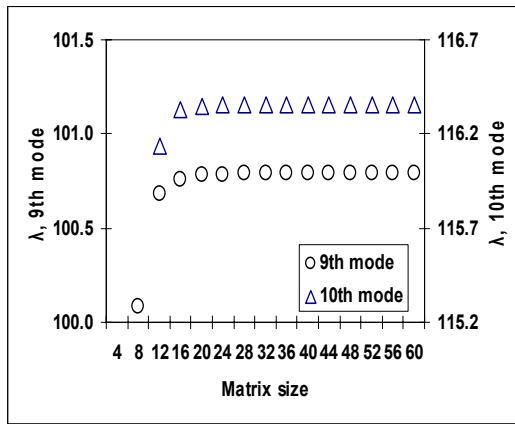
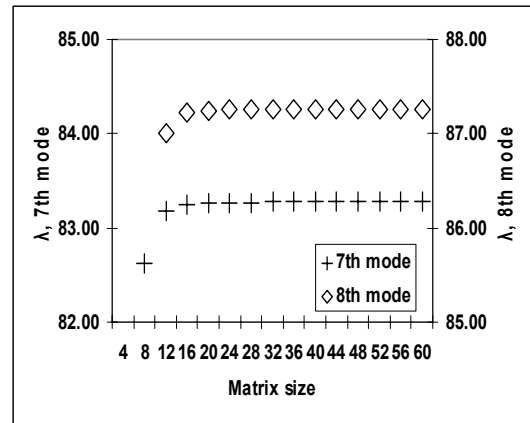
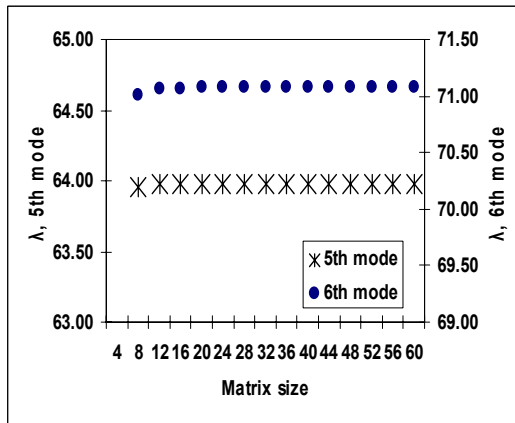
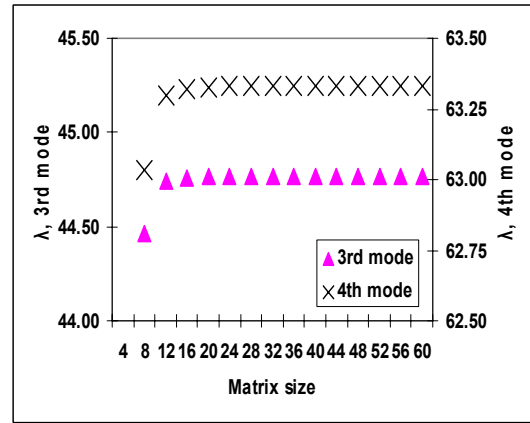
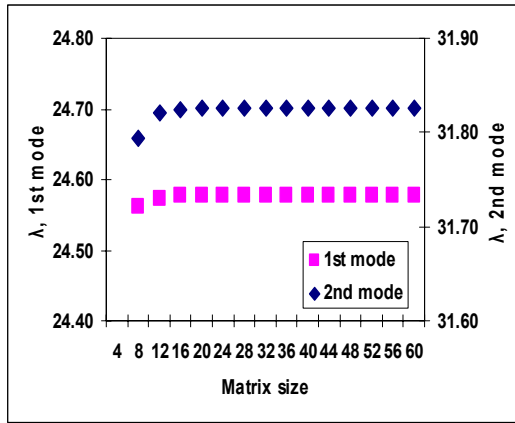


Figure 3.4 Convergence test for the eigenvalues of fully clamped rectangular plate computed by the superposition method ( $\Phi = 2.0$ )

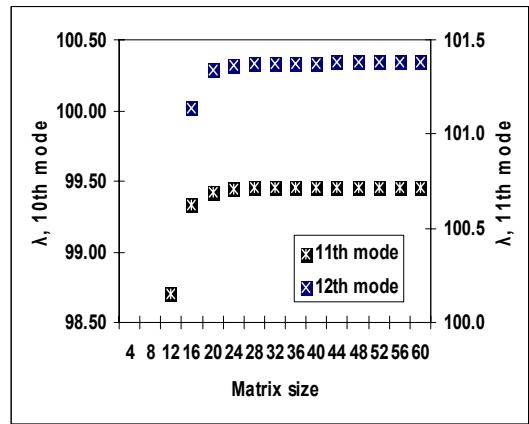
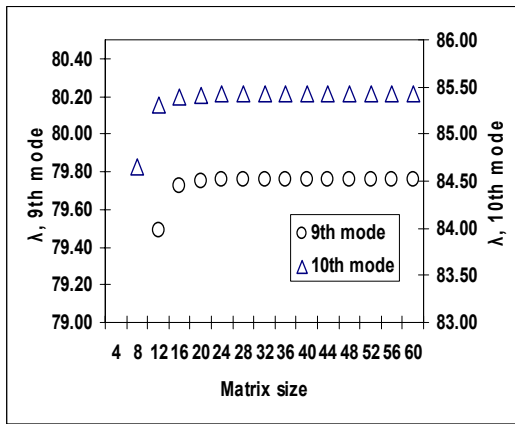
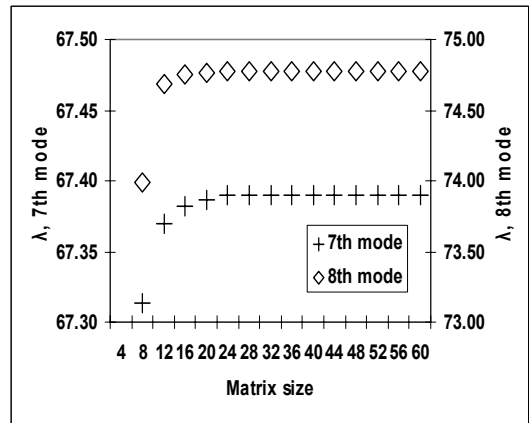
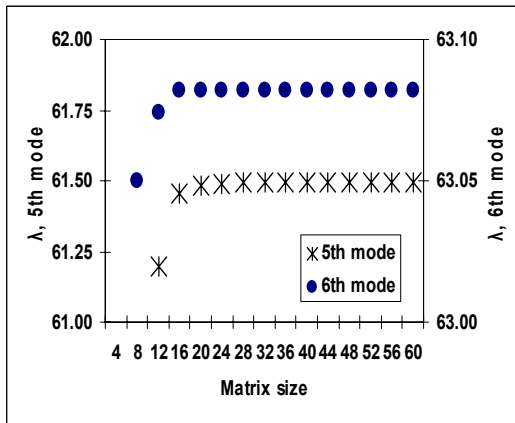
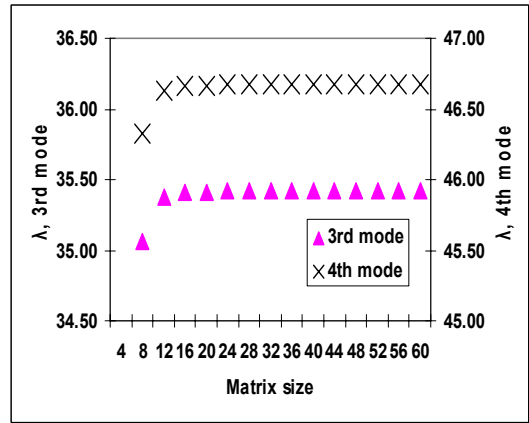
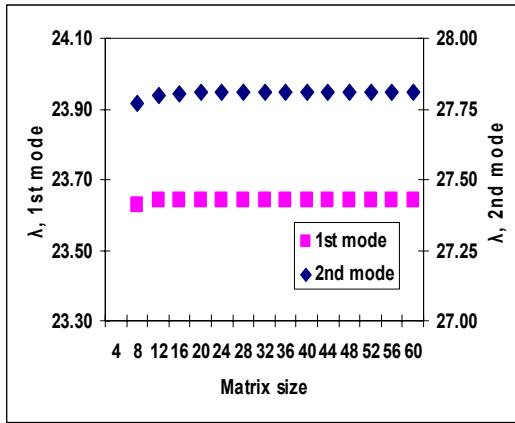


Figure 3.5 Convergence test for the eigenvalues of fully clamped rectangular plate computed by the superposition method ( $\Phi = 2.5$ )

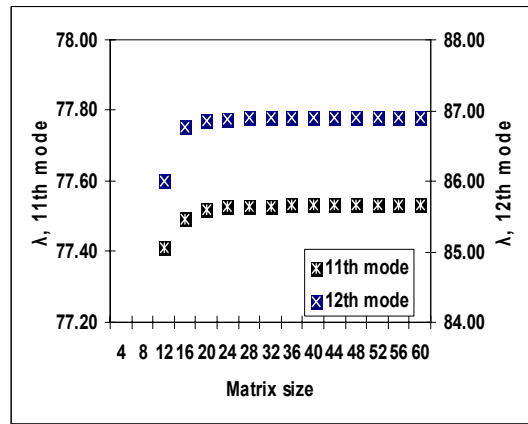
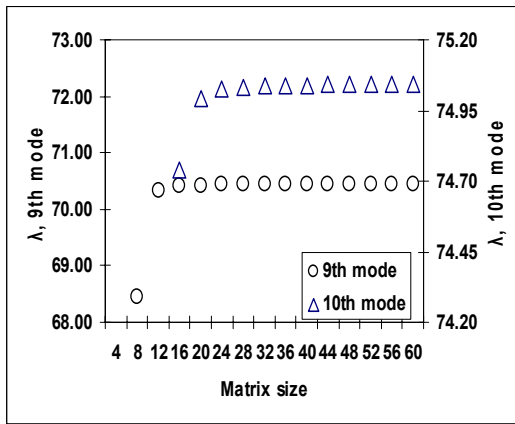
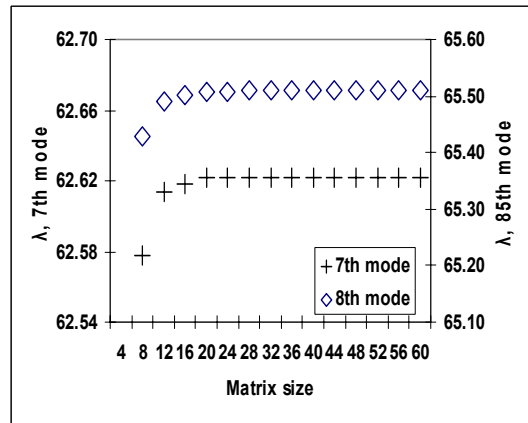
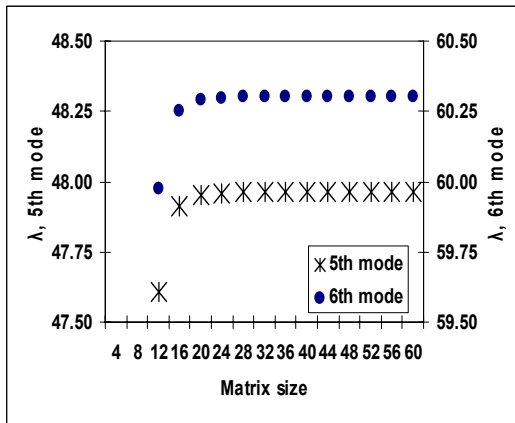
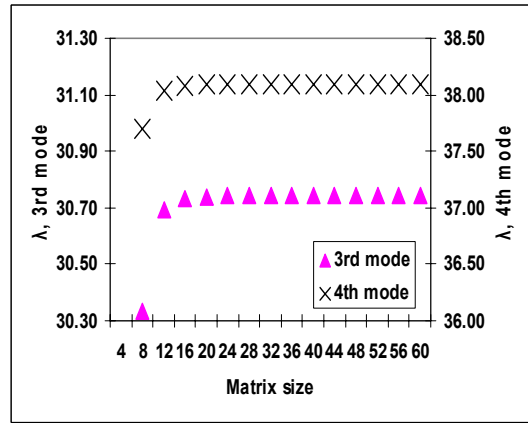
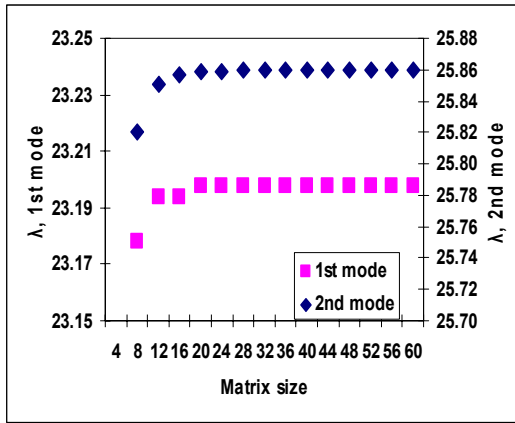


Figure 3.6 Convergence test for the eigenvalues of fully clamped rectangular plate computed by the superposition method ( $\Phi = 3.0$ )

### 3.1.2. Completely Free Plate

The first 12 eigenvalues of completely free plates with aspect ratios 1.0 to 3.0 obtained by the superposition method are shown in Table 3.2. The two letters adjacent to values express modal shapes. As with the case of the fully clamped plate, the eigenvalues in different family of modes were calculated separately. Making use of symmetry in the boundary conditions, the eigenvalues for the SS and AA modes need to be calculated for only aspect ratio  $\Phi$  of one or greater. For the SA modes, the aspect ratio varies from 1/3 to three due to lack of symmetry in the boundary conditions. The eigenvalues for SA mode for aspect ratio from 1/3 to one would be the same as those for AS modes of the plates with aspect ratio from three to one. All eigenvalues of the plate were computed with 15 terms.

Table 3.2 The eigenvalues of completely free plates obtained by the superposition method ( $\lambda^2 = \omega a^2 \sqrt{\rho/D}$ ,  $\nu = 0.3$ ).

Mode	$\Phi = b/a$					
	1		1.25		1.5	
1	13.47	AA	10.76	AA	8.931	AA
2	19.60	SS	13.59	SS	9.517	SS
3	24.27	SS	22.39	SS	20.60	SA
4	34.80		25.89	SA	22.18	SS
5	34.80	SA or AS	30.38	AS	25.65	AS
6	61.09		39.45	AS	29.79	AS
7	61.09	SA or AS	50.30	AA	38.16	AA
8	63.69	SS	51.49	SS	43.93	SS
9	69.27	AA	60.94	SA	53.35	SS
10	77.17	AA	69.49	AA	60.05	SA
11	105.5		76.58	SS	64.92	SA
12	105.5	SA or AS	80.48	AS	65.75	AS

Mode	$\Phi = b/a$					
	2		2.5		3	
1	5.366	SS	3.433	SS	2.382	SS
2	6.644	AA	5.278	AA	4.375	AA
3	14.62	SA	9.541	AS	6.617	AS
4	14.90	AS	11.33	SA	9.244	SA
5	22.00	SS	18.63	SS	13.03	SS
6	25.38	AA	18.92	AA	15.07	AA
7	26.00	AS	22.45	SS	21.31	AS
8	29.68	SS	24.44	AS	22.23	SS
9	36.04	SS	28.75	SA	22.29	SA
10	40.05	SA	31.45	SS	24.35	AS
11	48.45	AS	31.63	AS	28.67	SS
12	50.58	AS	41.22	AS	31.23	AA

### Convergence tests

The results of convergence tests for the eigenvalues of completely free plates with aspects ratios 1.0 to 3.0 obtained by the superposition are shown below. The rate of convergence is as fast as that of the fully clamped plates. No change is found in the fourth decimal place once the effective matrix size reaches  $20 \times 20$ .

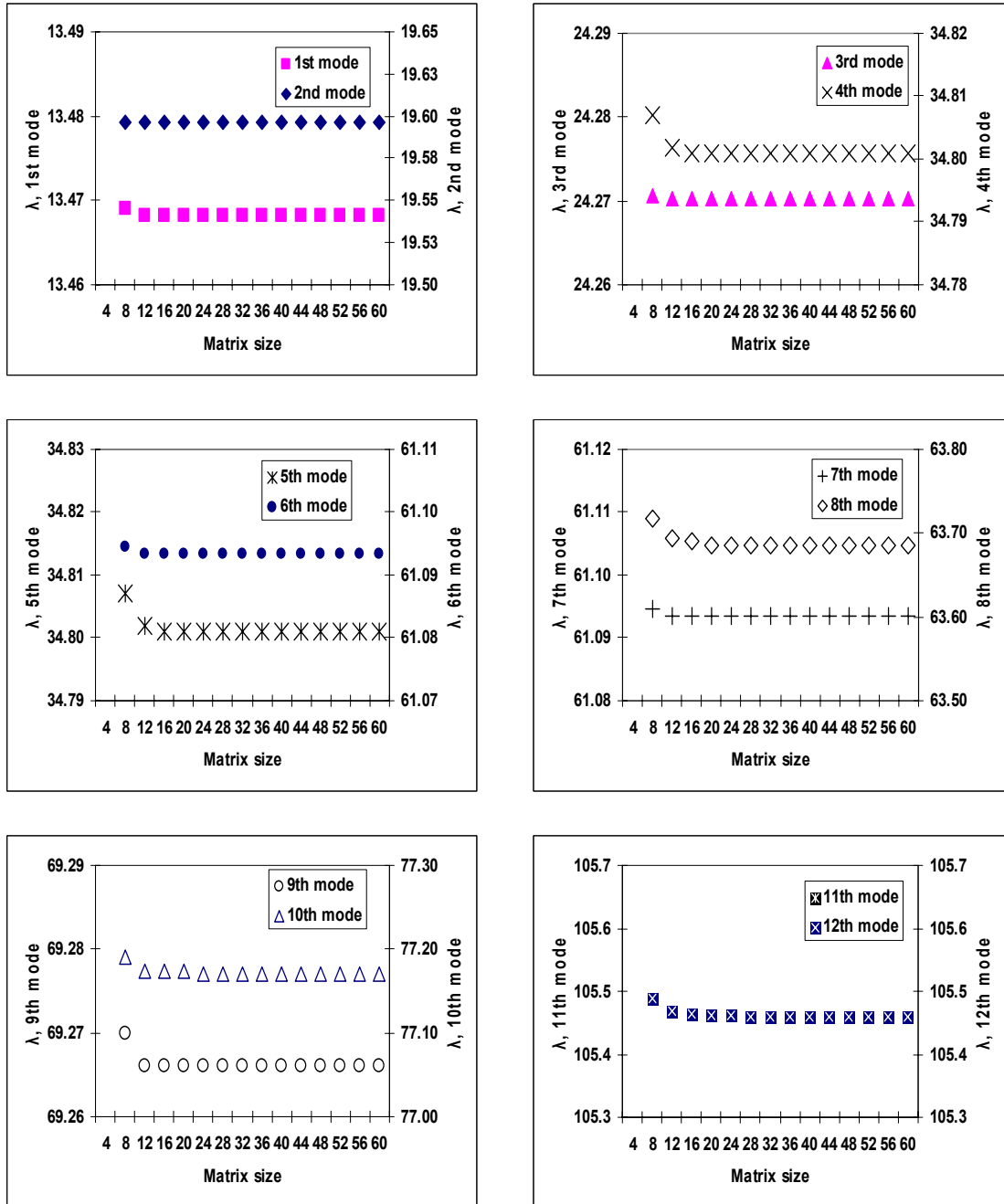


Figure 3.7 Convergence test for the eigenvalues of completely free rectangular plate computed by the superposition method ( $\Phi = 1.0$ )

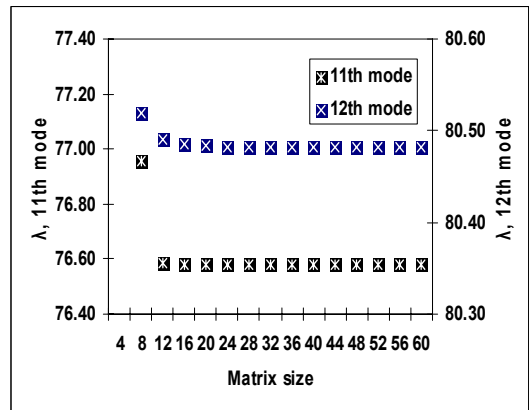
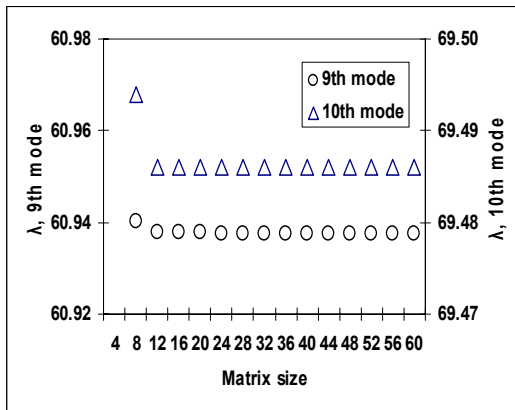
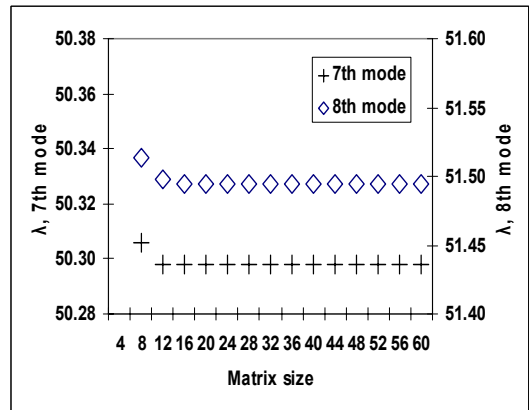
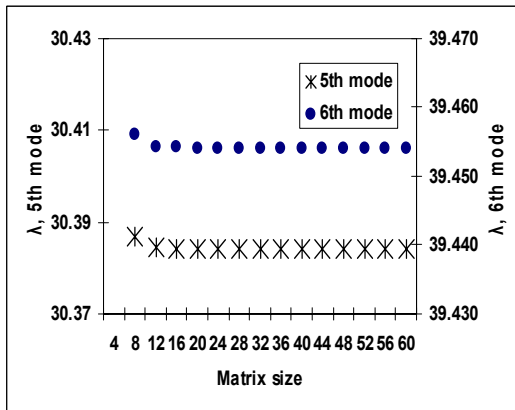
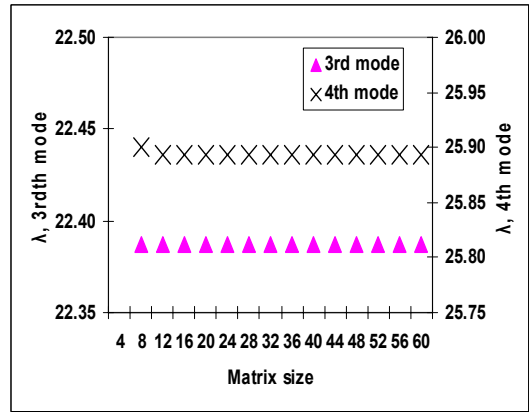
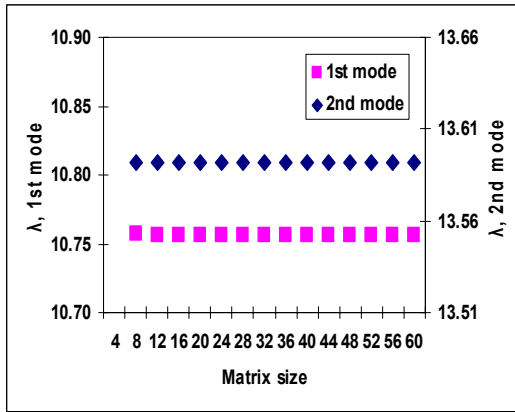


Figure 3.8 Convergence test for the eigenvalues of completely free rectangular plate computed by the superposition method ( $\Phi = 1.25$ )

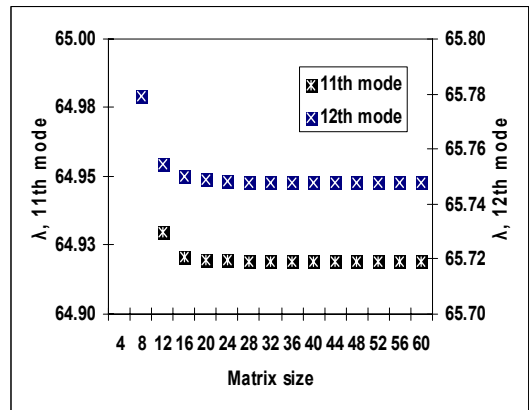
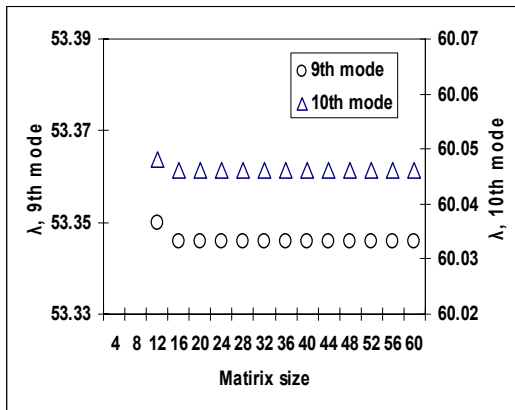
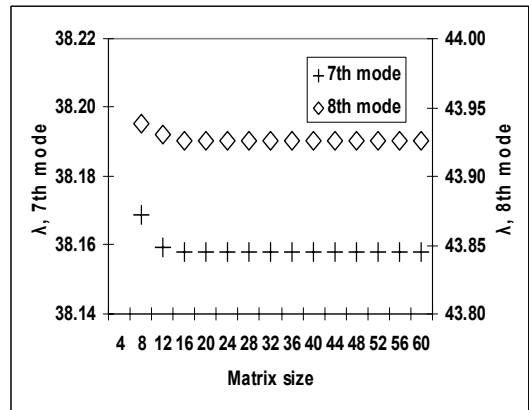
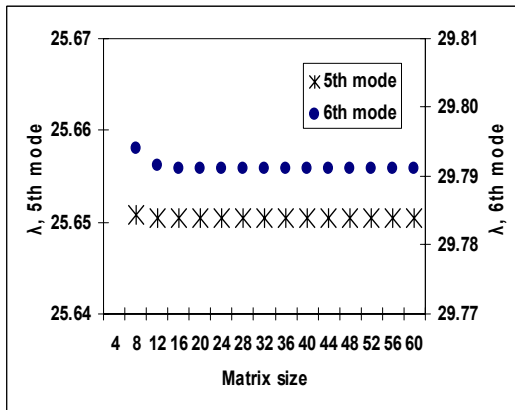
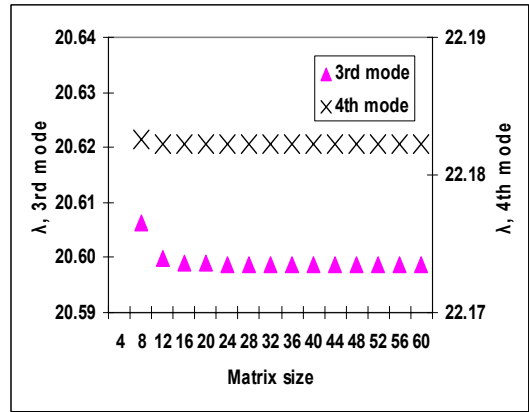
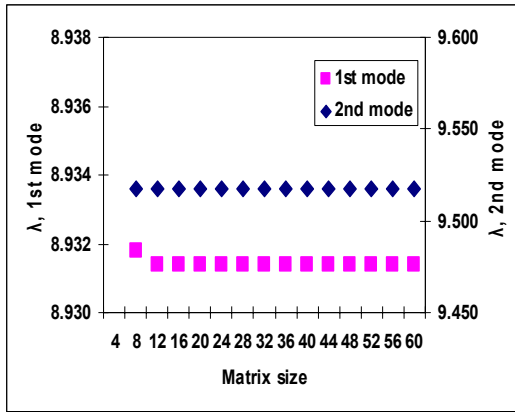


Figure 3.9 Convergence test for the eigenvalues of completely free rectangular plate computed by the superposition method ( $\Phi = 1.5$ )

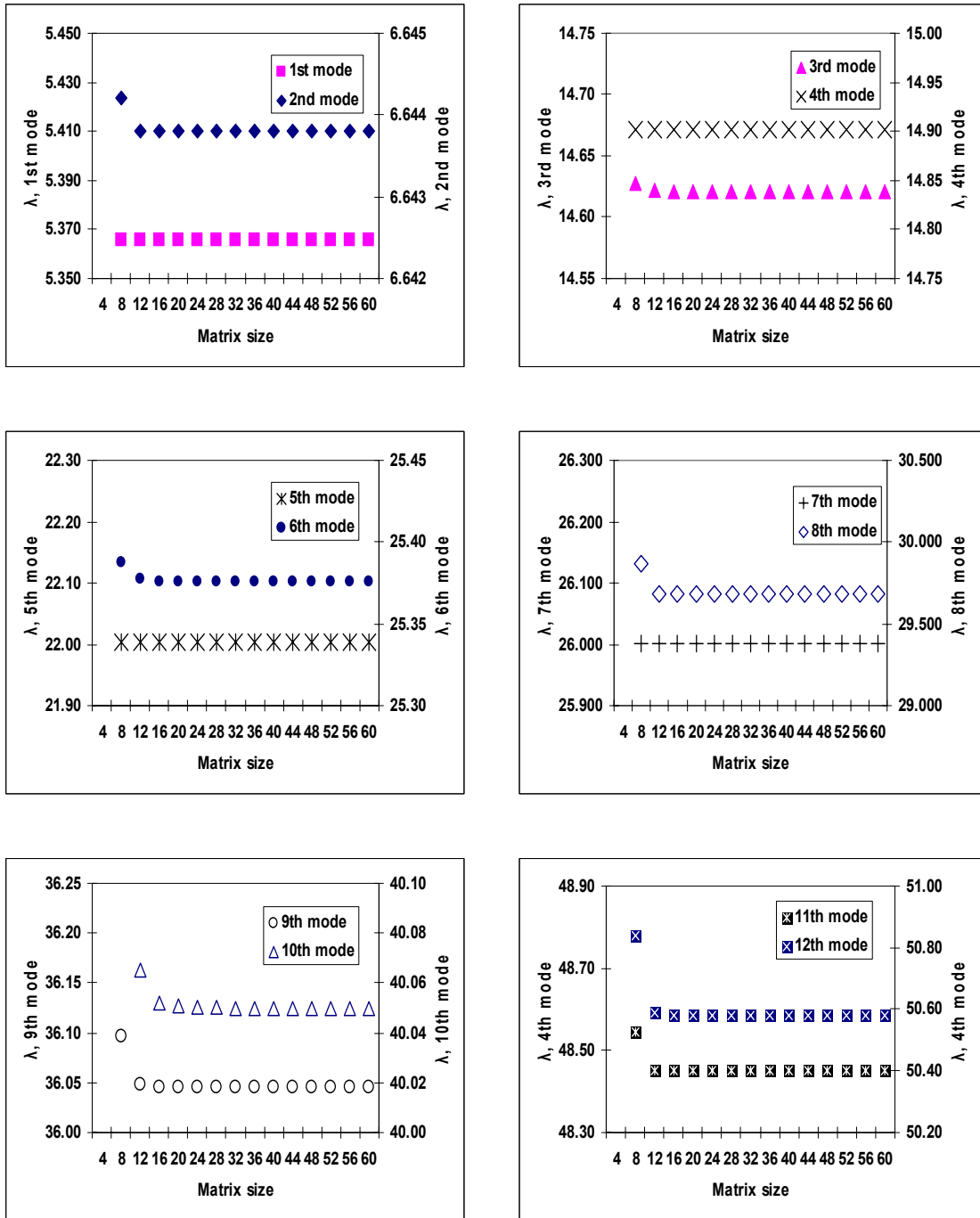


Figure 3.10 Convergence test for the eigenvalues of completely free rectangular plate computed by the superposition method ( $\Phi = 2.0$ )

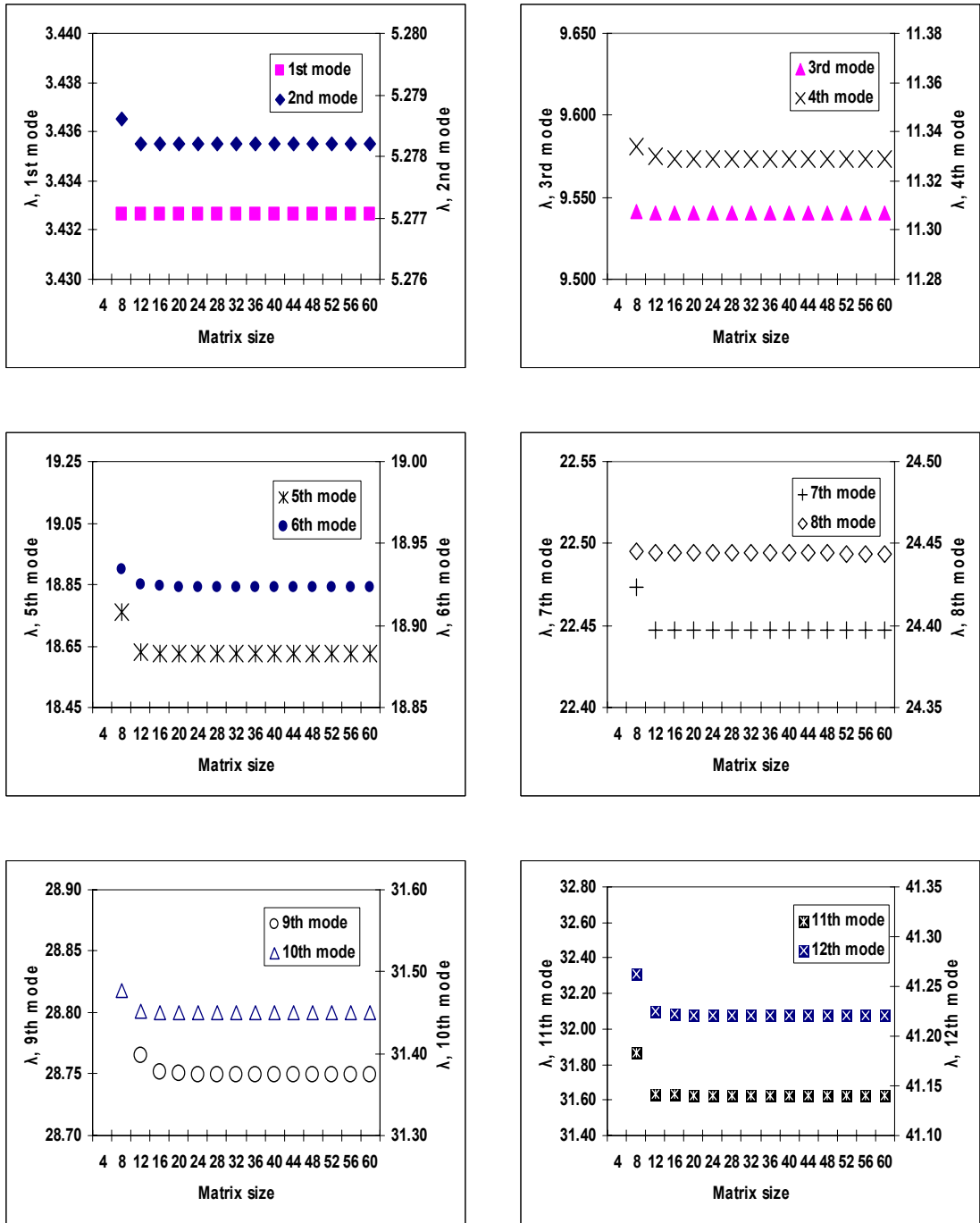


Figure 3.11 Convergence test for the eigenvalues of completely free rectangular plate computed by the superposition method ( $\Phi = 2.5$ )

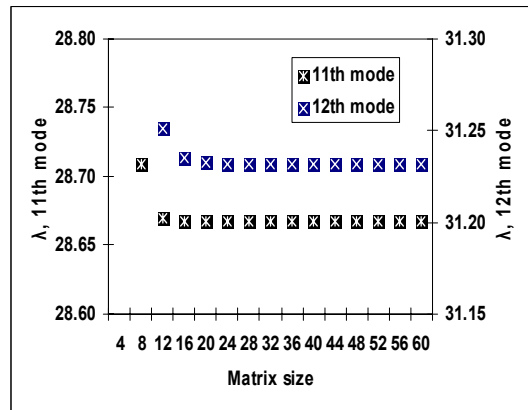
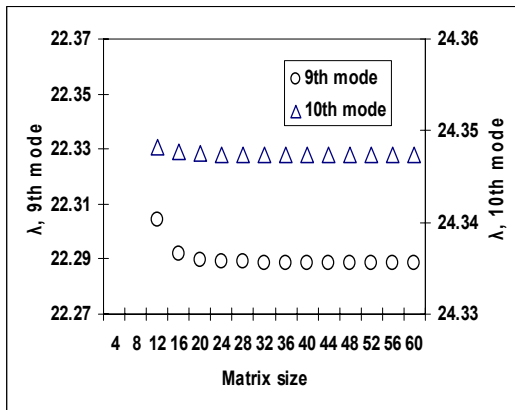
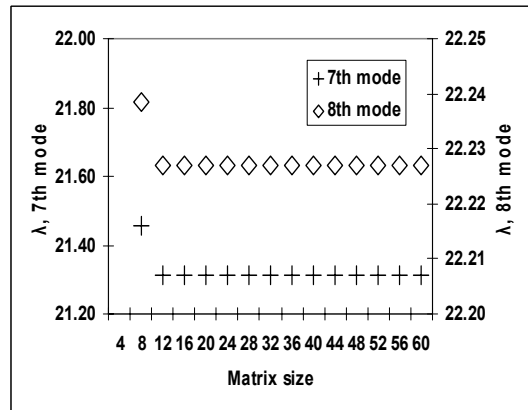
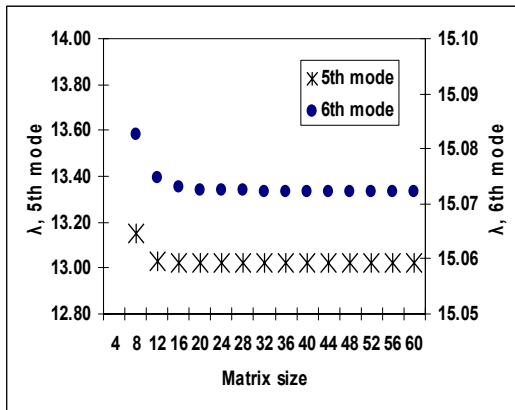
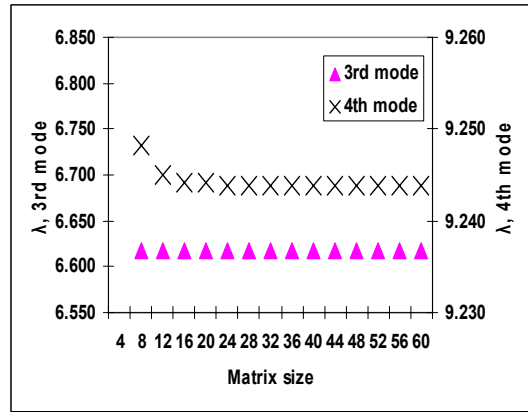
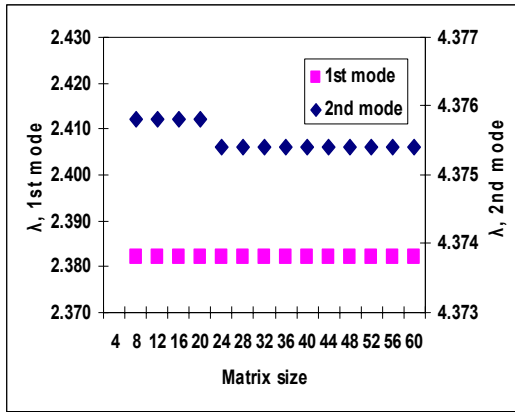


Figure 3.12 Convergence test for the eigenvalues of completely free rectangular plate computed by the superposition method ( $\Phi = 3.0$ )

## **3.2. *The Finite Difference Method***

From the convergence tests in the section of the fully clamped plates using the superposition method, the eigenvalues were found to be lower bounds as expected. As the objective of this thesis is to find both upper bound and lower bounds for the natural frequencies of those plates, and the lower bound values using the superposition method seem to be accurate enough, the eigenvalues of fully clamped plate calculated by using the FDM have been omitted. Therefore, only the eigenvalues of completely free plates are presented in this section.

### **3.2.1. Completely Free Plate**

The first 12 eigenvalues of completely free plates with aspect ratios 1.0 to 3.0 obtained by the FDM are shown in Table 3.3. The maximum number of nodes used to compute the eigenvalues is limited to  $55 \times 55$ , i.e. 3025 simultaneous equations to solve, because of the software's limitation.

Table 3.3 The eigenvalues of completely free plates obtained by the superposition method ( $\lambda^2 = \omega a^2 \sqrt{\rho/D}$ ,  $\nu = 0.3$ ).

Mode	$\Phi = b/a$					
	1		1.25		1.5	
1	13.46	AA	10.75	AA	8.926	AA
2	19.57	SS	13.57	SS	9.503	SS
3	24.24	SS	22.36	SS	20.57	SA
4	34.75		25.86	SA	22.15	SS
5	34.75	SA or AS	30.34	AS	25.58	AS
6	60.90		39.34	AS	29.73	AS
7	60.90	SA or AS	50.15	AA	38.05	AA
8	63.56	SS	51.39	SS	43.84	SS
9	69.04	AA	60.74	SA	53.07	SS
10	76.95	AA	69.27	AA	59.82	SA
11	105.1		76.17	SS	64.63	SA
12	105.1	SA or AS	80.23	AS	65.55	AS

Mode	$\Phi = b/a$					
	2		2.5		3	
1	5.358	SS	3.428	SS	2.379	SS
2	6.640	AA	5.275	AA	4.373	AA
3	14.60	SA	9.511	AS	6.596	AS
4	14.85	AS	11.31	SA	9.233	SA
5	21.97	SS	18.53	SS	12.96	SS
6	25.31	AA	18.87	AA	15.04	AA
7	25.96	AS	22.41	SS	21.16	AS
8	29.53	SS	24.40	AS	22.19	SS
9	35.97	SS	28.62	SA	22.19	SA
10	39.86	SA	31.38	SS	24.29	AS
11	48.16	AS	31.39	AS	28.60	SS
12	50.33	AS	40.96	AS	31.02	AA

### ***Convergence test***

The convergence tests were conducted for the eigenvalue of completely free plates with aspect ratio 1.0 to 3.0 obtained by the FDM as well. The results are shown below. As can be seen, all eigenvalues converge from below.

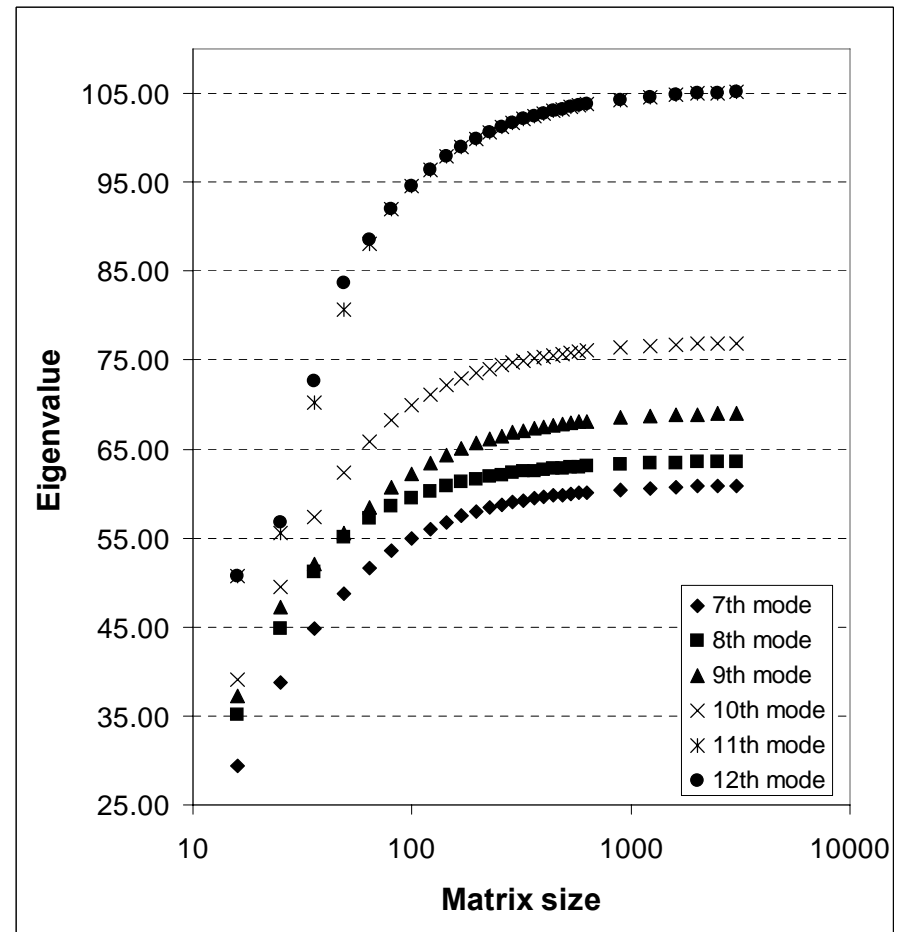
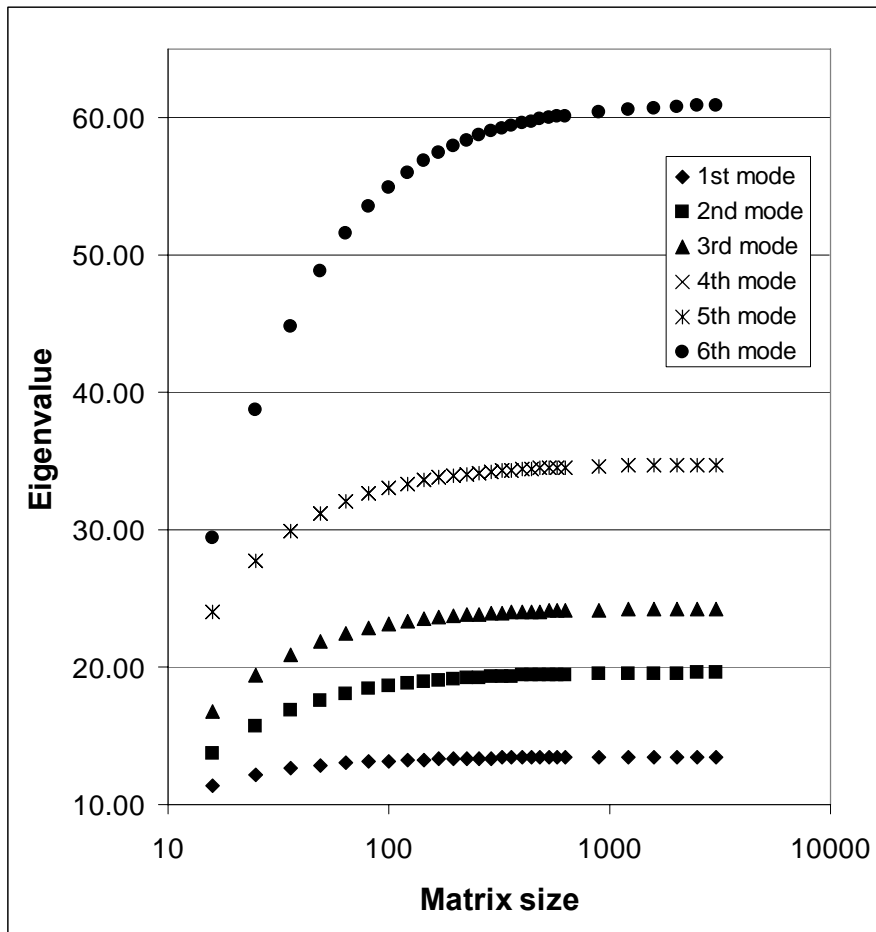


Figure 3.13 Convergence test for the eigenvalues of completely free rectangular plate computed by the finite difference method ( $\Phi = 1.0$ )

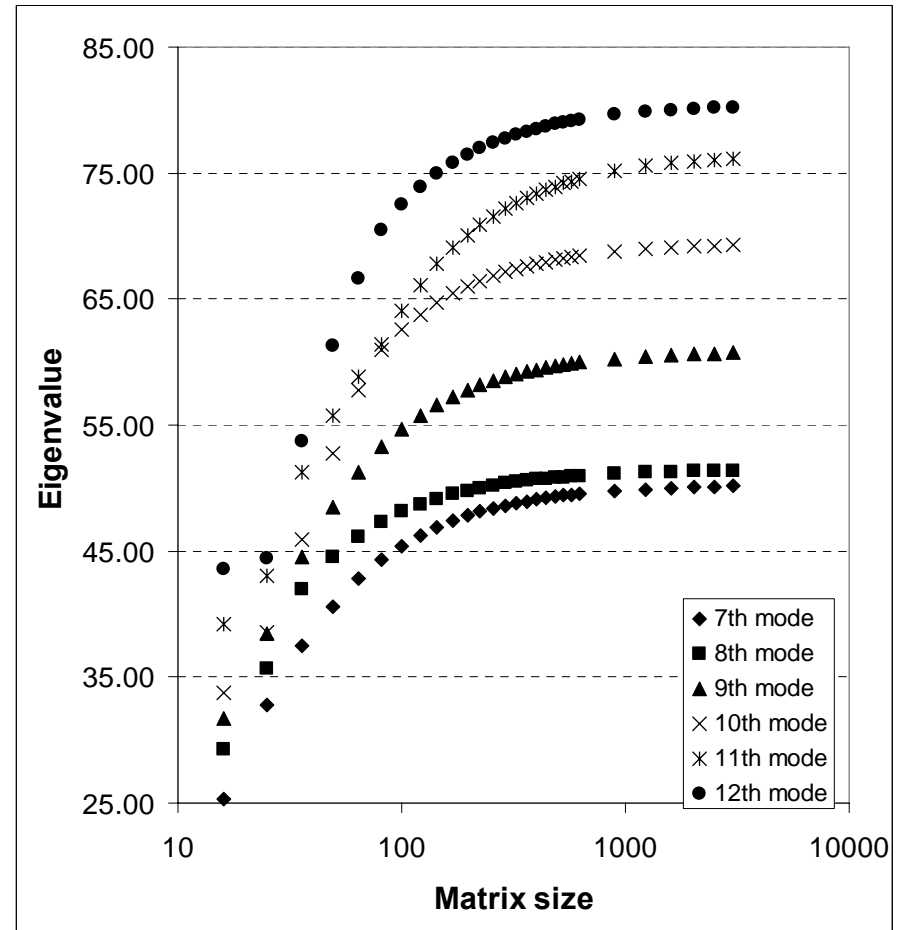
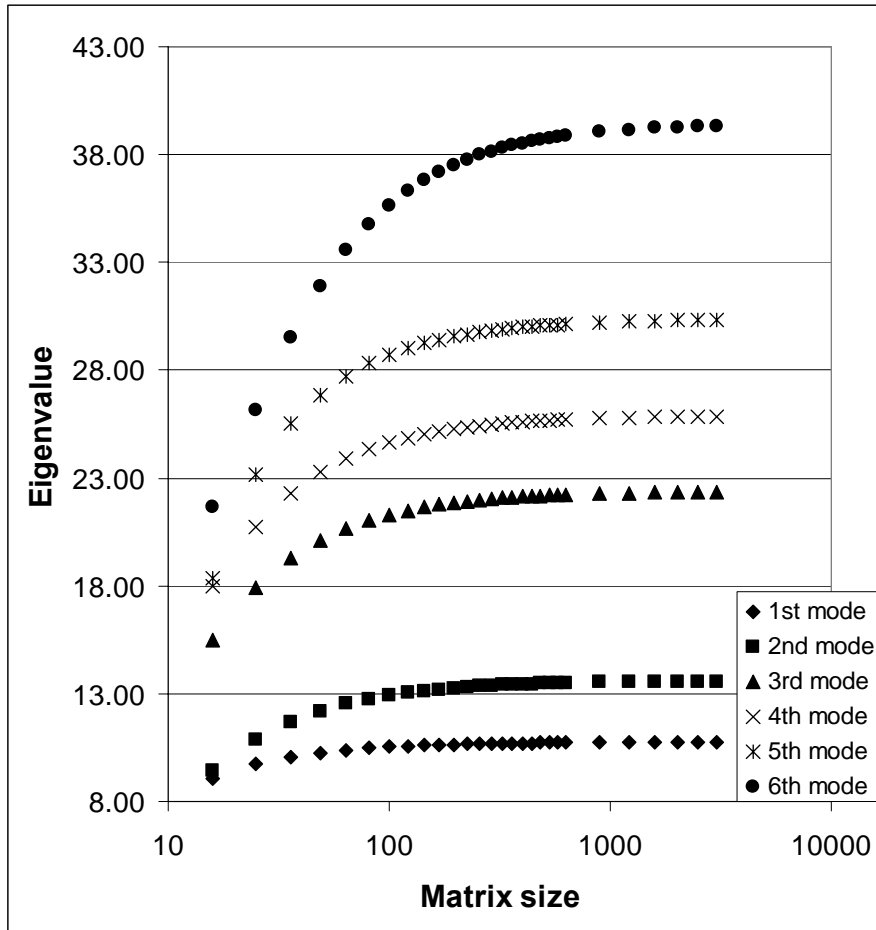


Figure 3.14 Convergence test for the eigenvalues of completely free rectangular plate computed by the finite difference method ( $\Phi = 1.25$ )

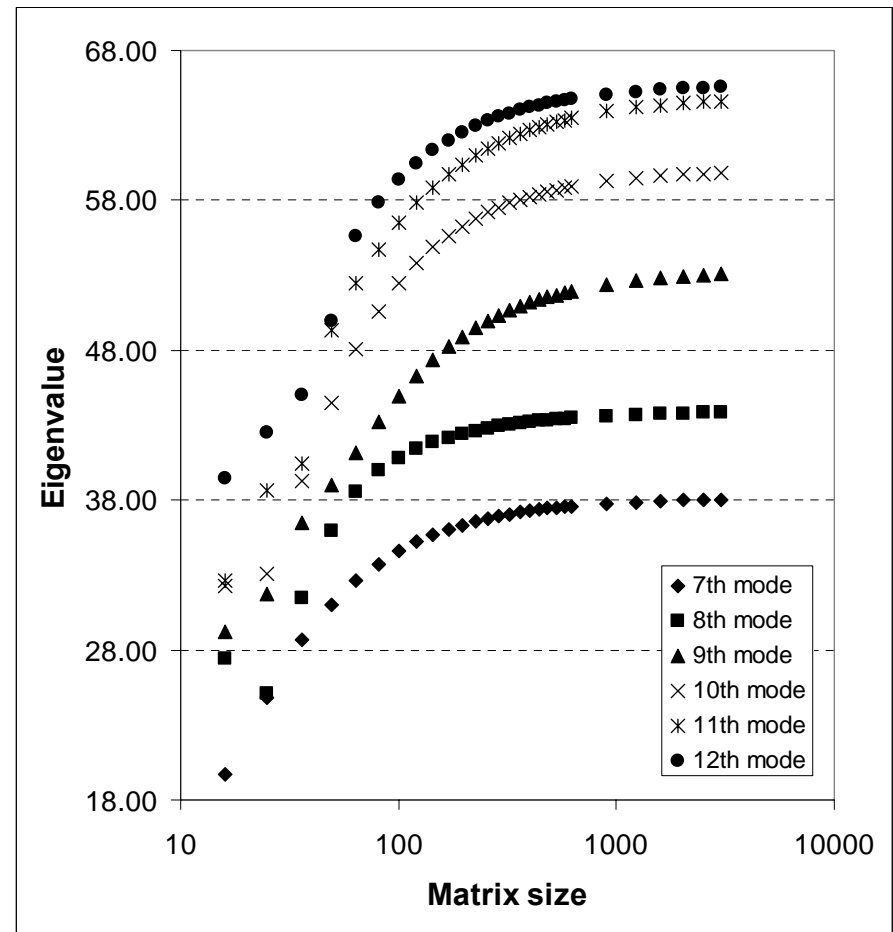
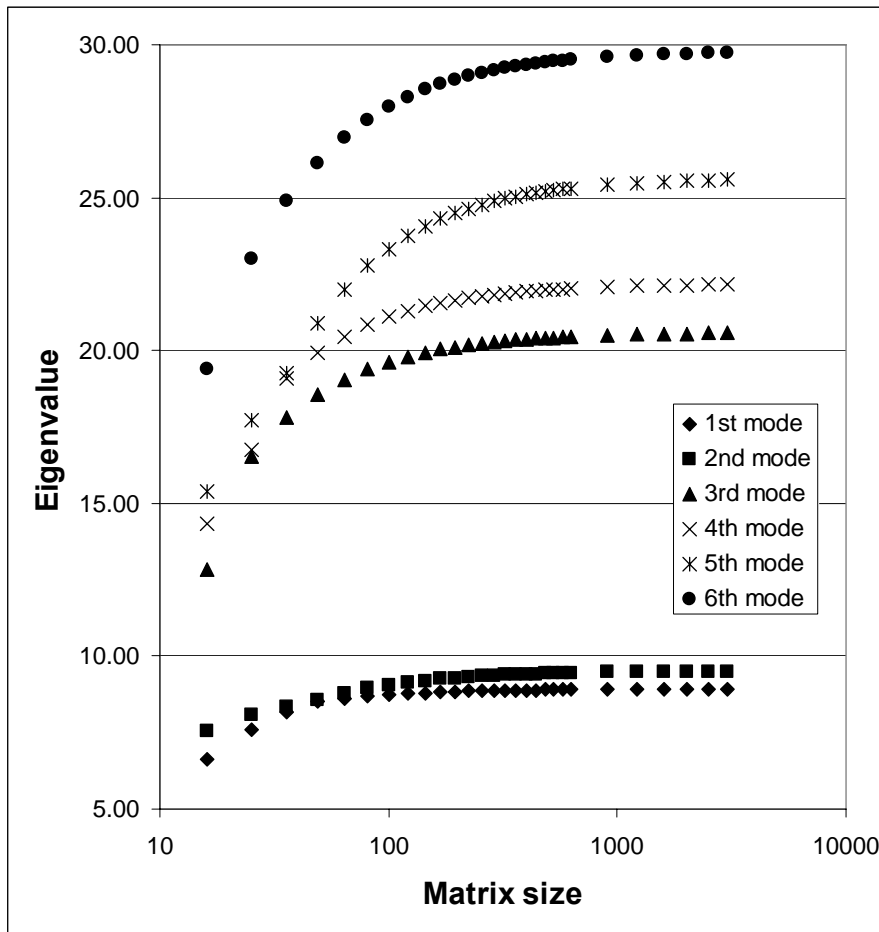


Figure 3.15 Convergence test for the eigenvalues of completely free rectangular plate computed by the finite difference method ( $\Phi = 1.5$ )

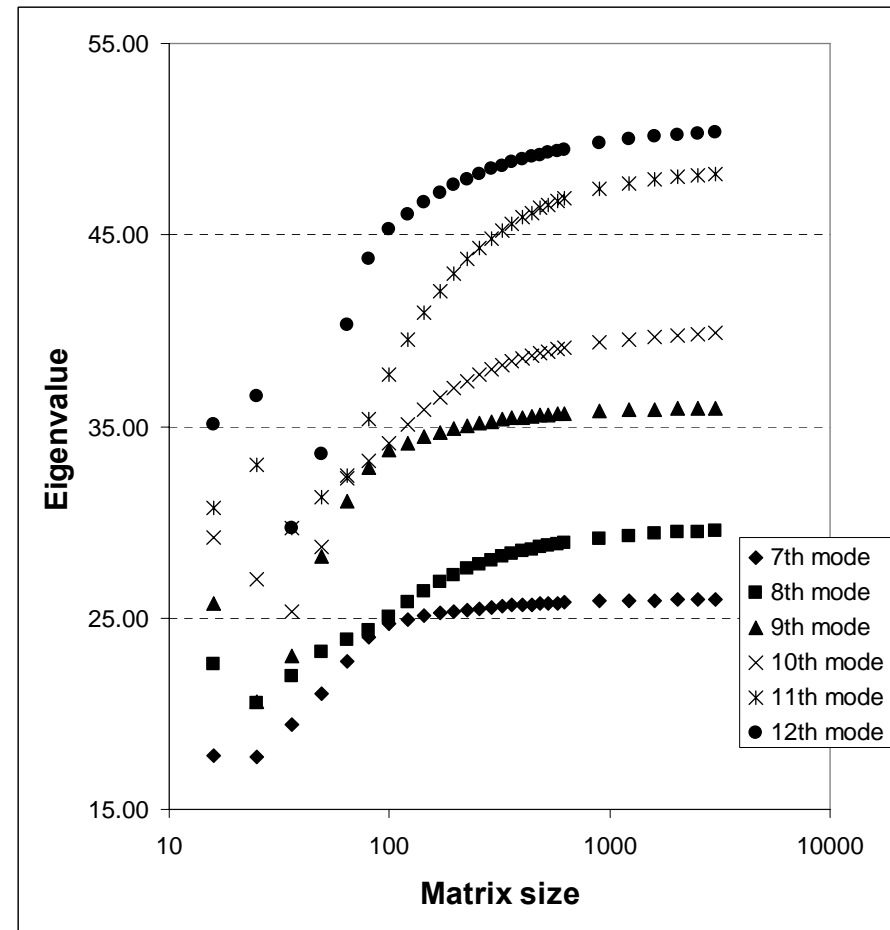
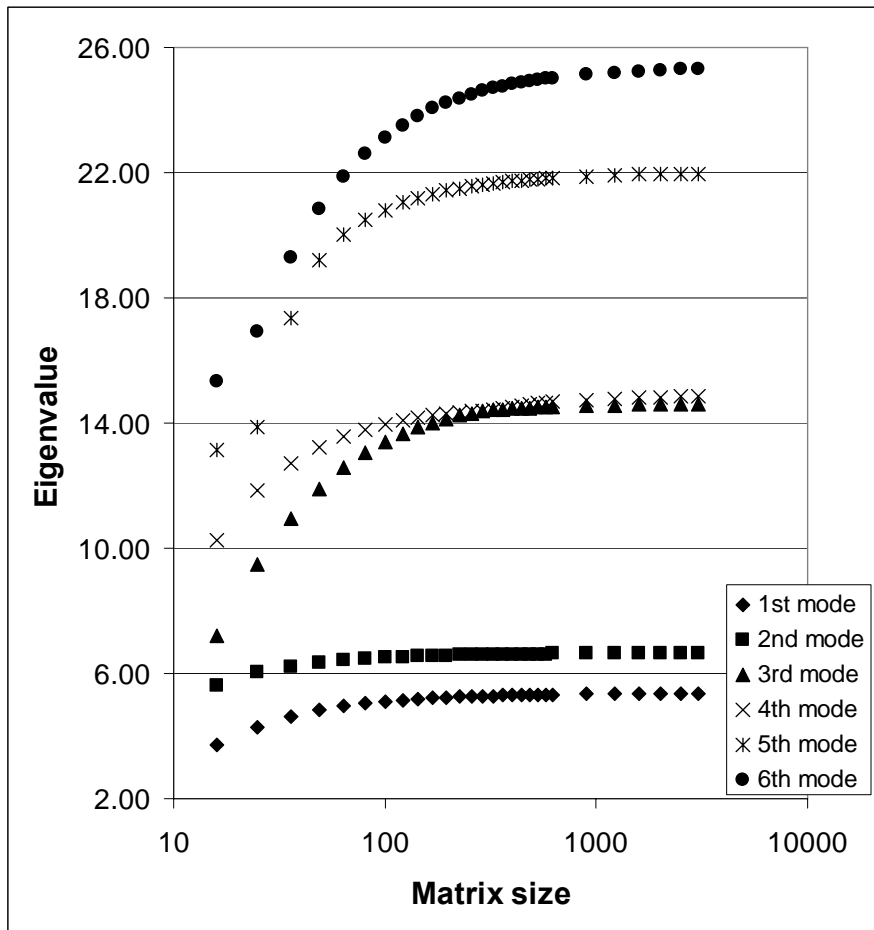


Figure 3.16 Convergence test for the eigenvalues of completely free rectangular plate computed by the finite difference method ( $\Phi = 2.0$ )

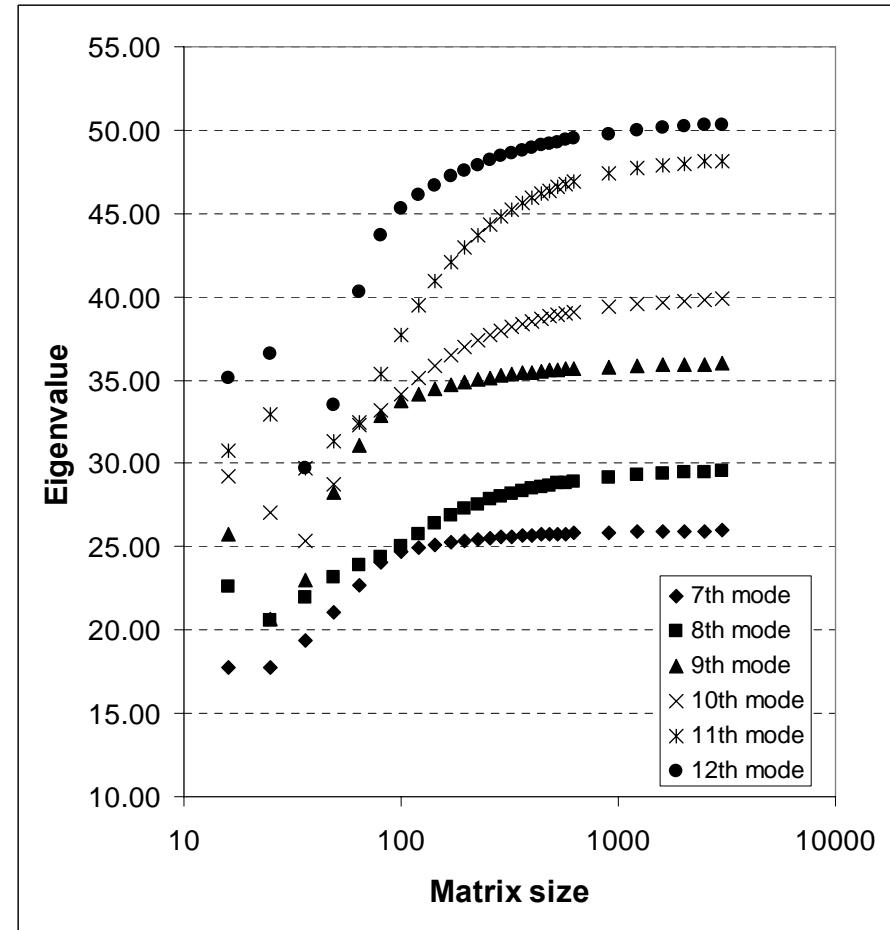
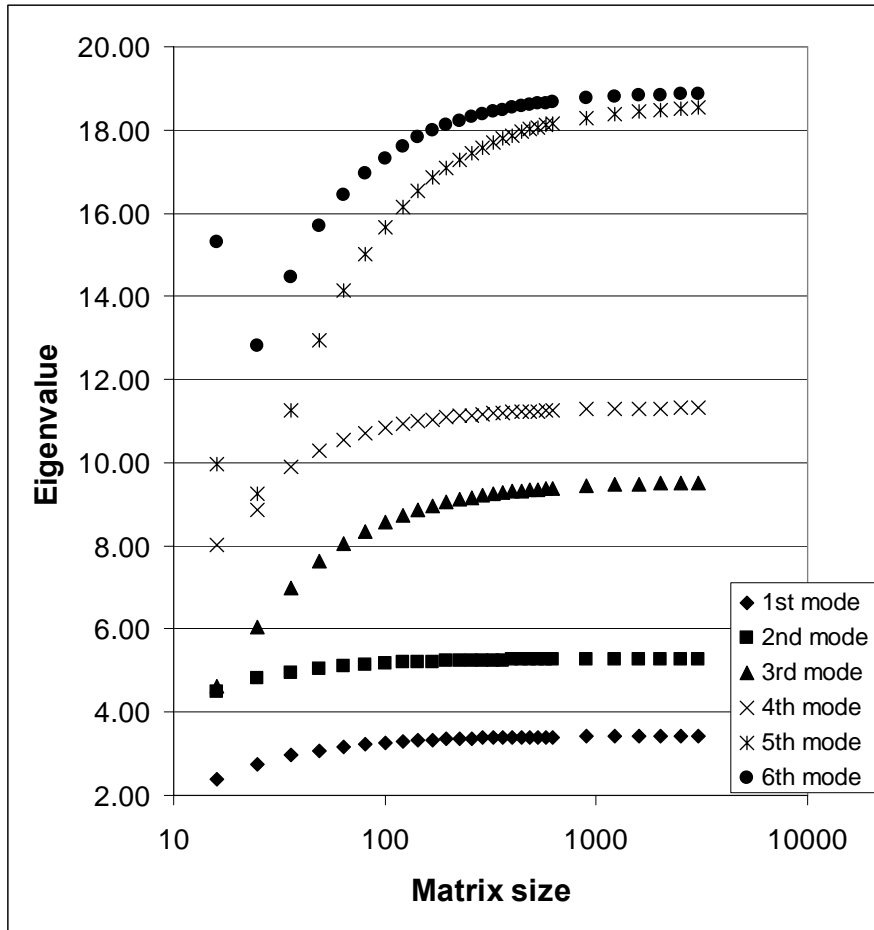


Figure 3.17 Convergence test for the eigenvalues of completely free rectangular plate computed by the finite difference method ( $\Phi = 2.5$ )

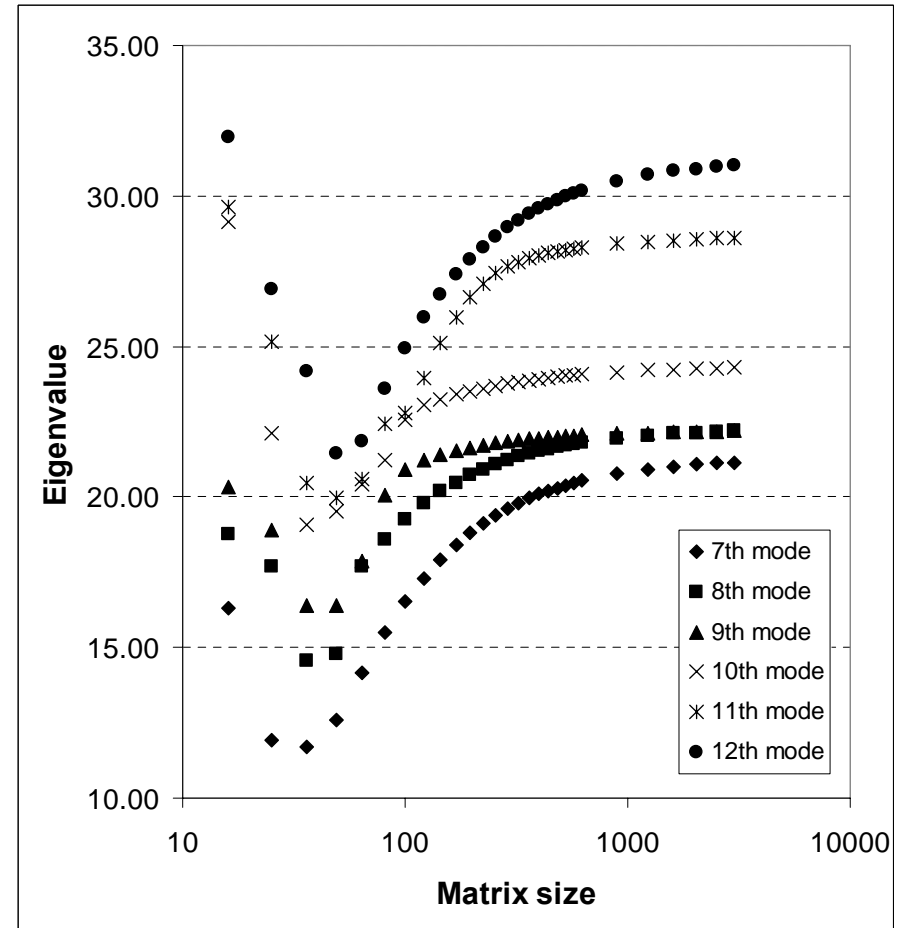
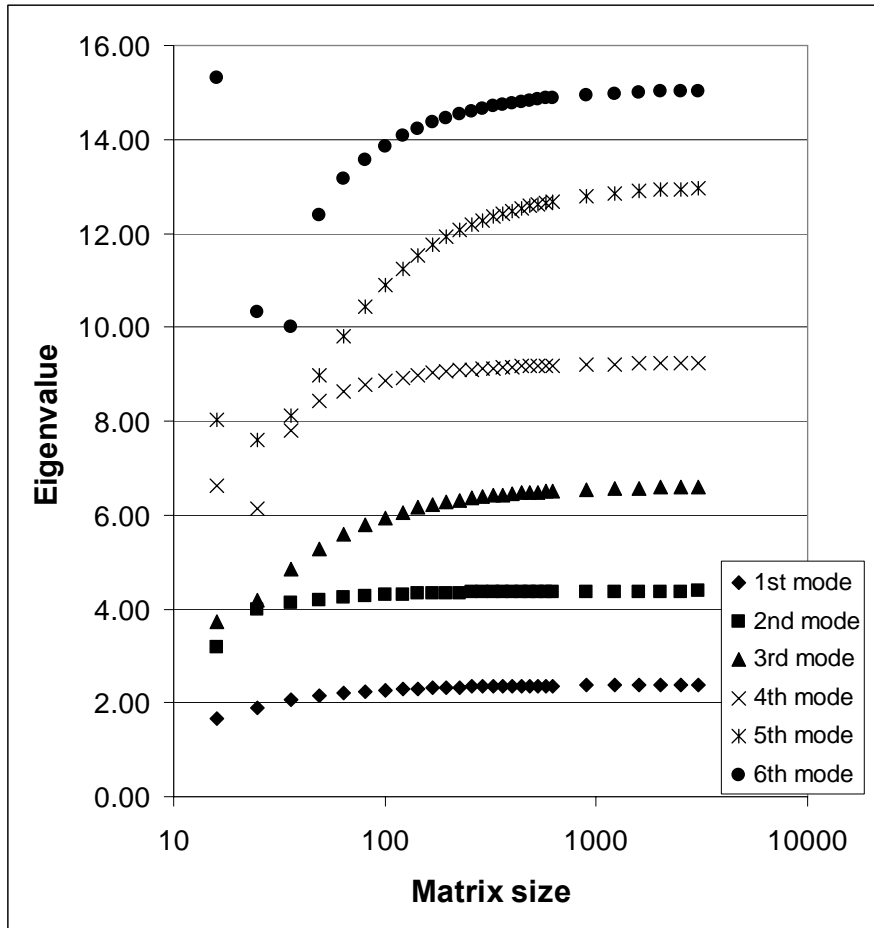


Figure 3.18 Convergence test for the eigenvalues of completely free rectangular plate computed by the finite difference method ( $\Phi = 3.0$ )

# **Chapter IV**

## **Discussion**

## 4. DISCUSSION

The free vibration analyses of the fully clamped and completely free rectangular plates were carried out by using the superposition method and the finite difference method (FDM). All calculated eigenvalues of both fully clamped and completely free plates converge as shown in the previous chapter. However, the direction of convergence in the superposition method depends on the boundary conditions of the actual plates and those of the building blocks, and there is a significant difference in the rate of convergence between the superposition method and the FDM.

### ***4.1. Fully Clamped Plate***

As Figure 3.1 to 3.6 shows, the eigenvalues of fully clamped plate computed by the superposition method converge as the matrix size is increased. The rate of convergence is remarkably rapid. All eigenvalues of the fully clamped plates have no change in fourth digit when the effective matrix size is more than  $28 \times 28$ . All of those convergences occur from below, which appear to be lower bounds. This confirms the prediction in a recent publication, which is that the superposition method would give a lower bound for the eigenvalues if its building blocks have more flexible boundary conditions than those of the system being modelled [4].

In the literature [1], first ten eigenvalues of the fully clamped plates for various aspect ratios are available, which are retrieved from Claassen and Thorne's publication [8]. Those values are expected to be upper bounds. Bazley, Fox and Stadter also give accurate upper bounds and lower bounds for the frequencies of doubly symmetric mode of fully clamped plates [9]. The eigenvalues obtained by the superposition method are compared with the values in reference [1] and shown in Table 4.1, which gives the upper bounds and lower bounds of natural frequencies of the fully clamped rectangular plates. There is almost no difference between the upper bounds and the lower bounds in fourth

digit number. This shows that exact results have been delimited accurately, in most cases to the fourth significant place.

Table 4.1 The lower bound and the upper bound for the eigenvalues of fully clamped rectangular plates with an aspect ratio of 1:3 ( $\lambda^2 = \omega a^2 \sqrt{\rho/D}$ ) [8],

\*: [9]

Mode	1			1.25			1.5		
	Lower bound (SM)	Upper bound [8]		Lower bound (SM)	Upper bound [8]		Lower bound (SM)	Upper bound [8]	
1	35.99	35.99	SS	29.89	29.89	SS	27.01	27.01	SS
2	73.39	73.39	SA or	52.51	52.51	AS	41.70	41.71	AS
3	73.39	73.39	AS	68.51	68.51	SA	66.13	66.13	SA
4	108.2	108.2	AA	89.25	89.26	SS	66.52	66.53	SS
5	131.6	131.6	SS	89.35	89.35	AA	79.81	79.81	AA
6	132.2	132.2	SS	124.3	124.3	SA	100.8	100.8	AS
7	165.0	165.0	SA or	127.5	127.5	SS	103.1	103.1	SA
8	165.0	165.0	AS	139.2	139.2	AS	125.3	125.3	SS
9	210.5	210.5	SA or	147.5	147.5	AS	136.1	136.1	AA
10	210.5		AS	173.0	173.0	AA	138.6	138.6	AS
11	220.0	*220.1	SS	181.3	*181.3	SS	144.2	*144.2	SS
12	242.2	242.2	AA	202.1	*202.1	SS	161.2	*161.2	SS

Mode	2			2.5			3		
	Lower bound (SM)	Upper bound [8]		Lower bound (SM)	Upper bound [8]		Lower bound (SM)	Upper bound [8]	
1	24.58	24.58	SS	23.64	23.64	SS	23.20	23.20	SS
2	31.83	31.83	AS	27.81	27.81	AS	25.86	25.86	AS
3	44.77	44.77	SS	35.42	35.42	SS	30.74	30.75	SS
4	63.33	63.33	AS	46.67	46.67	AS	38.09	38.11	AS
5	63.98	63.98	SA	61.49	61.50	SS	47.97	48.00	SS
6	71.08	71.08	AA	63.08	63.08	SA	60.30	60.35	AS
7	83.27	83.27	SA	67.39	67.39	AA	62.62	62.62	SA
8	87.25	87.25	SS	74.78	74.78	SA	65.51	65.51	AA
9	100.8	100.8	AA	79.76	79.76	AS	70.44	40.45	SA
10	116.4	116.4	AS	85.43	85.43	AA	75.04		SS
11	123.2	*123.3	SS	99.46		SA	77.53	77.55	AA
12	123.7		SA	101.4		SS	86.90		SA

## **4.2. Completely Free Plate**

Eigenvalues of the completely free plates for aspect ratios 1.0 to 3.0 were computed by using the superposition method and the FDM, and convergence tests were carried out for all the above aspect ratios and modes. Results of the tests are presented in Figure 3.7 through to Figure 3.18. As can be seen from these figures, both methods give results that converge as the matrix size is increased. The rate of convergence of the FDM is significantly slower than that of the superposition method but for all cases tested the convergence was from below as predicted by Weinberger [5]. However, the results of tests for the FDM show that some unexpected higher eigenvalues are found around small number of matrix size in Figure 3.16, 3.17 and 3.18. It is considered that the FDM does not give reliable results for higher modes with small number of nodes (coarse meshes) because there are not enough mesh points to express higher modal shapes.

The work shows that Gorman's superposition method gives excellent convergence in its results for the eigenvalue with only 20 terms. These results also confirm the prediction in a recent paper [4] that Gorman's results are expected to be upper bounds for a free plate. Thus the exact natural frequencies of a completely free plate are bracketed by the results of the method of superposition and the FDM. These results are shown in Table 4.2.

Table 4.2 The lower bound and the upper bound for the eigenvalues of completely free rectangular plates with an aspect ratio of 1:3

$(\lambda^2 = \omega a^2 \sqrt{\rho/D}, \nu = 0.3)$

Mode	1			1.25			1.5		
	Lower bound (FDM)	Upper bound (SM)		Lower bound (FDM)	Upper bound (SM)		Lower bound (FDM)	Upper bound (SM)	
1	13.46	13.47	AA	10.75	10.76	AA	8.926	8.931	AA
2	19.57	19.60	SS	13.57	13.59	SS	9.503	9.517	SS
3	24.24	24.27	SS	22.36	22.39	SS	20.57	20.60	SA
4	34.75	34.80	SA or	25.86	25.89	SA	22.15	22.18	SS
5	34.75	34.80	AS	30.34	30.38	AS	25.58	25.65	AS
6	60.90	61.09	SA or	39.34	39.45	AS	29.73	29.79	AS
7	60.90	61.09	AS	50.15	50.30	AA	38.05	38.16	AA
8	63.56	63.69	SS	51.39	51.49	SS	43.84	43.93	SS
9	69.04	69.27	AA	60.74	60.94	SA	53.07	53.35	SS
10	76.95	77.17	AA	69.27	69.49	AA	59.82	60.05	SA
11	105.1	105.5	SA or	76.17	76.58	SS	64.63	64.92	SA
12	105.1	105.5	AS	80.23	80.48	AS	65.55	65.75	AS

Mode	2			2.5			3		
	Lower bound (FDM)	Upper bound (SM)		Lower bound (FDM)	Upper bound (SM)		Lower bound (FDM)	Upper bound (SM)	
1	5.358	5.366	SS	3.428	3.433	SS	2.379	2.382	SS
2	6.640	6.644	AA	5.275	5.278	AA	4.373	4.375	AA
3	14.60	14.62	SA	9.511	9.541	AS	6.596	6.617	AS
4	14.85	14.90	AS	11.31	11.33	SA	9.233	9.244	SA
5	21.97	22.00	SS	18.53	18.63	SS	12.96	13.03	SS
6	25.31	25.38	AA	18.87	18.92	AA	15.04	15.07	AA
7	25.96	26.00	AS	22.41	22.45	SS	21.16	21.31	AS
8	29.53	29.68	SS	24.40	24.44	AS	22.19	22.23	SS
9	35.97	36.04	SS	28.62	28.75	SA	22.19	22.29	SA
10	39.86	40.05	SA	31.38	31.45	SS	24.29	24.35	AS
11	48.16	48.45	AS	31.39	31.63	AS	28.60	28.67	SS
12	50.33	50.58	AS	40.96	41.22	AS	31.02	31.23	AA

In Table 4.3, the eigenvalues obtained by using the FDM are compared with the results published in Leissa's review [1]. The upper bound and lower bound results by Leissa were taken from [10]. It is seen that the results of the FDM are lower than published upper bounds but higher than the lower bounds. The present results are higher than the previously published lower bounds and very close to the upper bounds indicating these may be the best lower bound solutions available to date.

Table 4.3 Comparison of eigenvalues obtained by the FDM with those in Leissa's monograph [1] for the doubly antisymmetric modes of the square free plate ( $\nu = 0.3$ )

Present	Leissa[1]	
	Lower bound	Upper bound
$b/a = 1$		
13.46	13.092	13.474
69.04	66.508	69.576
76.95	75.146	77.411
$b/a = 1.25$		
10.75	10.479	10.761
50.15	48.352	50.487
69.27	67.665	69.746
$b/a = 1.5$		
8.926	8.6667	8.9351
38.05	36.651	38.294
66.50	64.844	66.965
$b/a = 2$		
6.640	6.4563	6.6464
25.31	24.417	25.455
58.32	56.151	59.051

# **Chapter V**

## **Conclusion and Recommendations**

## 5. CONCLUSION and RECOMMENDATIONS

The eigenvalues of fully clamped and completely free rectangular plates with various aspect ratios were computed by using the superposition method and the finite difference method (FDM). The upper bounds and lower bounds for the eigenvalues of these plates were successfully obtained.

The superposition method has given the lower bound for the eigenvalues of fully clamped plates. Almost no difference was noted between these values and those upper bound values in the early literature but the superposition method converged significantly faster than all other procedures.

The results by the FDM appear to be the best lower bounds for the eigenvalues of completely free rectangular plates available so far, and there is excellent agreement between these results and those upper bound values found by the superposition method. The exact results for the completely free plates have therefore been bracketed between these results. The FDM results seem to converge to exact eigenvalues of the plates as the mesh size approaches to zero. The rate of convergence, however, is slower than that of the superposition method.

The FDM does not give reliable results for higher modes with small number of nodes (coarse meshes) because there are not enough mesh points to express higher modal shapes. The maximum number of nodes used to compute the eigenvalues is limited to  $55 \times 55$  due to the software or memory limitations. It is expected that closer values to exact eigenvalues of the plate would be obtained if more nodes are used. The work also shows that Gorman's superposition method gives excellent convergence for the eigenvalues with only 20 terms.

The results presented in this thesis could be useful to give an estimate of the maximum possible error in the values of the natural frequencies of fully clamped and completely free plates.

The methods used in this thesis can also be applied to more complex vibration problems, for example, orthotropic plates, shells and also for the determination of buckling loads. It is recommended that where possible the superposition method be used to obtain eigenvalues because of its rapid rate of

convergence and accuracy. It is also recommended that further research be carried out to investigate the possibility of using the superposition method for the determination of eigenvalues of more complicated systems such as shells.

## References

- [1] A. W. Leissa, *Vibration of plates*: NASA SP-160, 1969.
- [2] D. J. Gorman, *Free vibration analysis of rectangular plates*. New York: Elsevier North Holland, 1982.
- [3] D. J. Gorman, "Free vibration analysis of the completely free rectangular plate by the method of superposition," *Journal of Sound and Vibration*, vol. 57, pp. 437-447, 1978.
- [4] S. Ilanko, "On the bounds of Gorman's superposition method of free vibration analysis," *Journal of Sound and Vibration*, vol. 294, pp. 418-420, 2006.
- [5] H. F. Weinberger, "Lower bounds for higher eigenvalues by finite difference methods," *Pacific Journal of Mathematics*, vol. 8, pp. 339-368, 1958.
- [6] G. D. Smith, *Numerical solution of partial differential equations: Finite difference method*, 3 ed. New York: Oxford University Press, 1985.
- [7] S. Ilanko, "The vibration behaviour of in-plane loaded rectangular plates," in *Department of Civil Engineering, Faculty of Science*, M.Sc. thesis. Manchester: University of Manchester, 1981.
- [8] R. W. Claassen and C. J. Thorne, "Transverse vibration of thin rectangular isotropic plates," NOTS Tech. Pub. 2379, NAVWEEPS Rept. 7016 U. S. Naval Ordnance Test Sta., China Lake, Calif., 1960.
- [9] N. W. Bazley, D. W. Fox, and J. T. Stadter, "Upper and lower bounds for the frequencies of rectangular clamped plates," Tech. Memo TG-626, Appl. Phys. Lab., The Johns Hopkins Univ., 1965.
- [10] N. W. Bazley, D. W. Fox, and J. T. Stadter, "Upper and lower bounds for the frequencies of rectangular free plates," *Journal of applied mathematics and physics*, vol. 18, pp. 445-460, 1967.
- [11] L. G. Jaeger, *Elementary theory of elastic plates*. New York: Pergamon Press, 1964.

## Appendix I: Theory of Thin Rectangular Plate

The elementary theory of the elastic bending of beams is well known. This leads in the case of pure bending about principal axes to the familiar formula,  $M = -EI \frac{d^2w}{dx^2}$ , where  $M$  is the bending moment,  $E$  Young's modulus,  $w$  the transverse deflection and  $x$  the longitudinal co-ordinate. A similar relationship can be obtained for a plate.

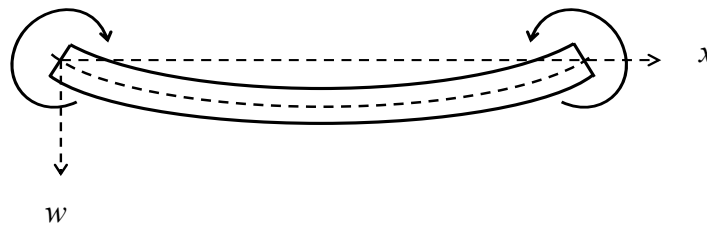


Figure A1. 1. The elastic bending of a beam

In Elementary theory of elastic plates [11], Jaeger presents a comprehensive and a simple deviation of the plate bending theory. For convenience and completeness, the relevant parts are presented here. Consider the case of a rectangular plate subjected to distributed moments, shown in Figure A1. 2. Considering an infinitesimal element of the plate (Figure A1. 3a), the middle surface is taken as the neutral surface and it is assumed that the cross section (plane perpendicular to the middle surface) still remain flat after bending (Figure A1. 3b). Then, the longitudinal strains in both  $x$  and  $y$  directions;  $\epsilon_x$  and  $\epsilon_y$  are proportional to the distance  $z$  from the neutral surface. For the elastic behaviour, stress is, therefore, also proportional to  $z$ .

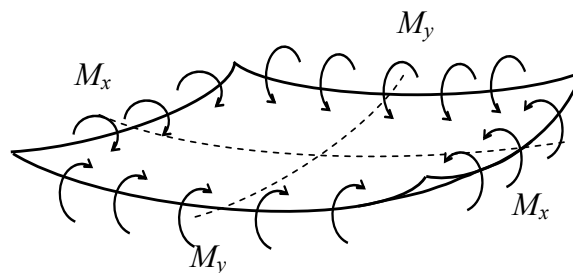


Figure A1. 2 A rectangular plate subjected to distributed moments

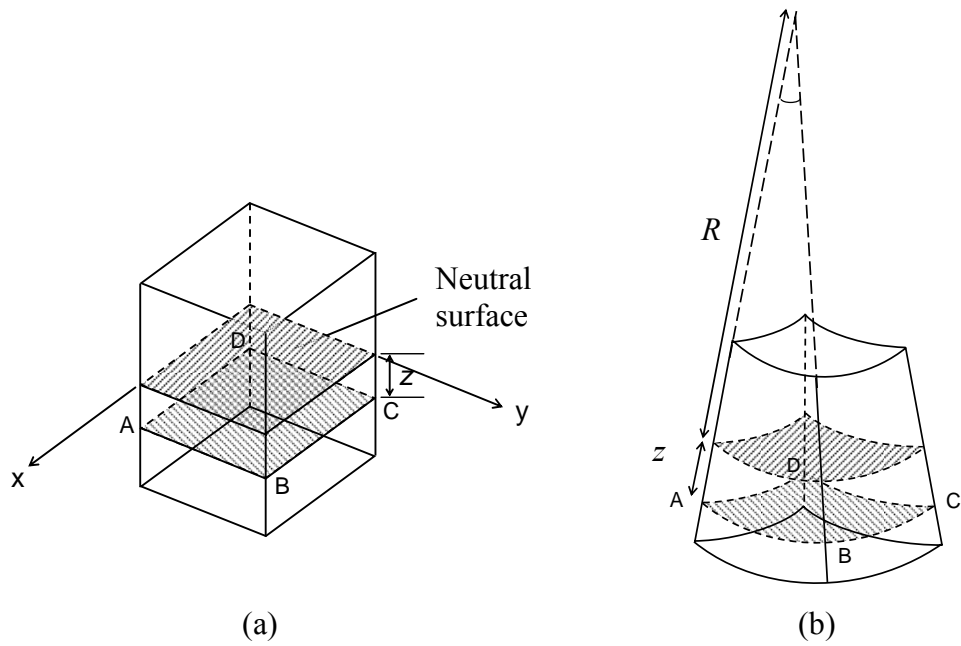


Figure A1. 3 A small piece of the plate

If a distributed moment  $M_x$  is applied on the plate only through normal stress distribution in the direction parallel to the  $y$  axis (Figure A1. 4a), the stresses at the surface ABCD will be given by  $\sigma_x = kz$ ,  $\sigma_y = 0$ , where  $k$  is some constant (Figure A1. 4b). The constant  $k$  can be found by equating the applied moment  $M_x$  to the resisting elastic moment per unit length. This gives

$$M_x = \int_{-h/2}^{h/2} kz^2 dz = \frac{kh^3}{12}, \text{ and so } k = \frac{12M_x}{h^3} \quad (\text{A1.1})$$

where  $h$  is the plate thickness.

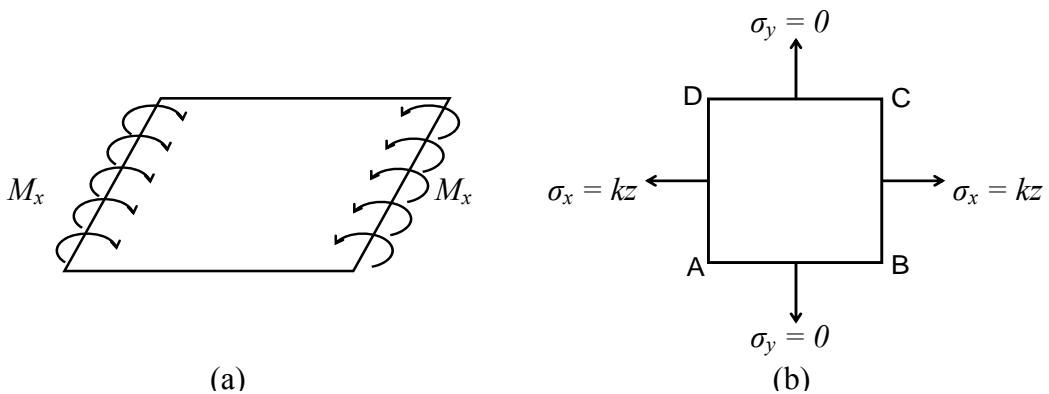


Figure A1. 4 The plate applied a distributed moment only in the direction parallel to the  $y$  axis

The stress  $\sigma_x$  is also given by  $\sigma_x = E\varepsilon_x$ , where  $\varepsilon_x$  is the strain in the  $x$  direction.

This gives,

$$\sigma_x = \frac{12M_x}{h^3} z = E\varepsilon_x \quad (\text{A1.2})$$

From Figure A1. 3b,  $\varepsilon_x$  will be

$$\varepsilon_x = \frac{(R+z)\theta - R\theta}{R\theta} = \frac{z}{R} \quad (\text{A1.3})$$

From Equations A1.2 and A1.3

$$\frac{1}{R} = \frac{12M_x}{Eh^3} \quad (\text{A1.4})$$

For small deflections,  $\frac{1}{R} = -\frac{\partial^2 w}{\partial x^2}$ , then

$$\frac{\partial^2 w}{\partial x^2} = -\frac{12M_x}{Eh^3} \quad (\text{A1.5})$$

There will also be a strain in the  $y$  direction due to the Poisson's ratio effect. The strain  $\varepsilon_y$  should be given by  $\varepsilon_y = -\nu\varepsilon_x$ , where  $\nu$  is the Poisson's ratio. This leads to the following relationship.

$$\frac{\partial^2 w}{\partial y^2} = \nu \frac{12M_x}{Eh^3} \quad (\text{A1.6})$$

From the relationship of Equations A1.5 and A1.6, if the distributed moment  $M_x$  is applied on the plate in the direction parallel to the  $y$  axis, it will produce the curvature of the plate not only in the  $xw$  plane but also in the perpendicular plane  $yw$ . The curvature in the  $yw$  plane is  $\nu$  times of the curvature in the  $xw$  plane and of opposite sign. Thus a sagging moment of  $M_x$  per unit length produces sagging curvature in the  $xw$  plane and hogging curvature in  $yw$  plane as shown in Figure A1. 5.

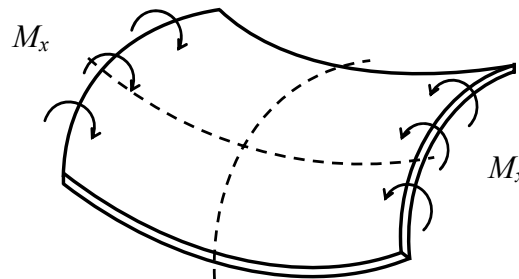


Figure A1. 5 The plate applied a sagging moment

From the above argument and using the principle of superposition, it is possible to obtain the curvature of the plate when applying moments per unit length  $M_x$  and  $M_y$  simultaneously. The contribution of  $M_x$  and  $M_y$  to the curvature in the  $xw$  plane are  $12M_x/Eh^3$  and  $-v12M_y/Eh^3$  respectively.

Hence,

$$-\frac{\partial^2 w}{\partial x^2} = \frac{12}{Eh^3} (M_x - vM_y) \quad (\text{A1.7a})$$

Similarly

$$-\frac{\partial^2 w}{\partial y^2} = \frac{12}{Eh^3} (M_y - vM_x) \quad (\text{A1.7b})$$

Rearranging Equations A1.7, the moment  $M_x$  and  $M_y$  will be expressed in terms of the curvature as follows.

$$M_x = -D \left( \frac{\partial^2 w}{\partial x^2} + v \frac{\partial^2 w}{\partial y^2} \right) \quad (\text{A1.8a})$$

and

$$M_y = -D \left( \frac{\partial^2 w}{\partial y^2} + v \frac{\partial^2 w}{\partial x^2} \right) \quad (\text{A1.8b})$$

where  $D = \frac{Eh^3}{12(1-\nu^2)}$  and it is called the plate rigidity.

So far the situation where only the bending moment applied on the plate was considered. In general, equilibrium of plate requires the presence of bending and twisting moment in any direction. In the following part, the general case will be examined and the relationship between twisting moments and twisting curvatures will also be established.

Bending moments  $M_x$  and  $M_y$ , and twisting moment  $M_{xy}$  are applied to a plate (Figure A1. 6a). Considering the equilibrium of the wedge, some bending moment  $M_n$  and twisting moment  $M_{nt}$  are acting on arbitrarily chosen plane as shown in Figure A1. 6b. Let the  $n, t$  axes be at an angle  $\alpha$  to the  $x, y$  axes.

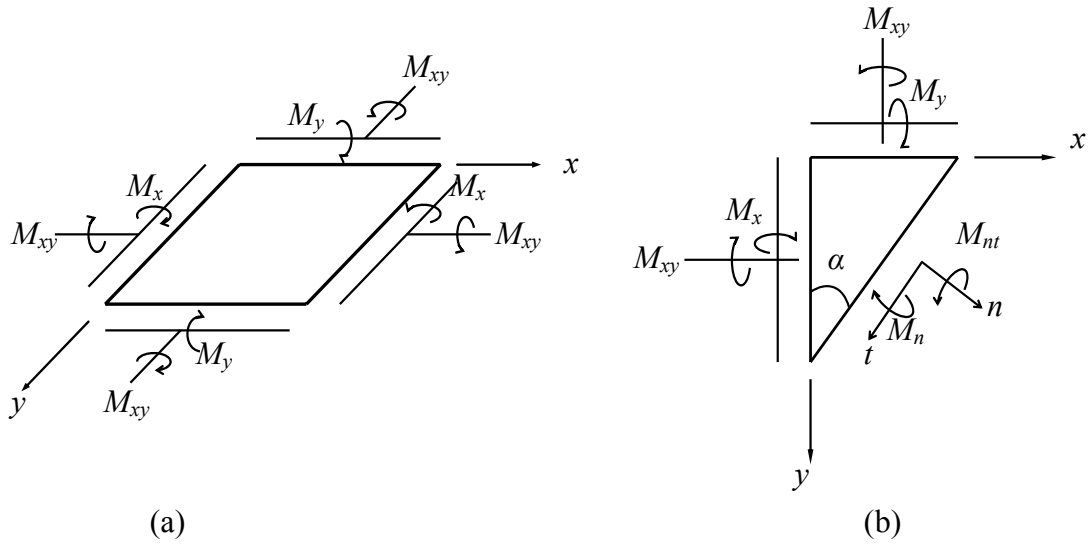


Figure A1. 6 The plate bending moments  $M_x$  and  $M_y$ , and twisting moment  $M_{xy}$  are applied

Taking moment around the  $t$  axis then gives,

$$\begin{aligned}
 M_n &= M_x \cos^2 \alpha + M_y \sin^2 \alpha - 2M_{xy} \sin \alpha \cos \alpha \\
 &= \left( \frac{M_x + M_y}{2} \right) + \left( \frac{M_x - M_y}{2} \right) \cos 2\alpha - M_{xy} \sin 2\alpha
 \end{aligned} \tag{A1.9a}$$

Similarly taking moments about the  $n$  axis gives,

$$\begin{aligned}
 M_{nt} &= M_x \sin \alpha \cos \alpha - M_y \sin \alpha \cos \alpha + M_{xy} (\cos^2 \alpha - \sin^2 \alpha) \\
 &= \left( \frac{M_x - M_y}{2} \right) \sin 2\alpha + M_{xy} \cos 2\alpha
 \end{aligned} \tag{A1.9b}$$

To obtain maximum or minimum of  $M_n$ , let  $\frac{\partial M_n}{\partial \alpha} = 0$ , then

$$-2 \left( \frac{M_x - M_y}{2} \right) \sin 2\alpha - 2M_{xy} \cos 2\alpha = 0 \tag{A1.9c}$$

Thus

$$\tan 2\alpha = \frac{-2M_{xy}}{(M_x - M_y)} \tag{A1.9d}$$

It should be noted that from Equations A1.9b and c,  $M_{nt}$  will be zero when  $M_n$  is maximum or minimum. The twisting moment is absent only on these two orthogonal sections, which are called principal sections. The form of Equations A1.9c and d are identical with that obtained when considering stress at a point and finding direct and shear stresses in various directions. The bending moment and

twisting moments at a point in a plate may therefore be represented on a Mohr's circle as shown in Figure A1. 7.

From Equation A1.9d

$$\sin 2\alpha = \frac{-2M_{xy}}{\sqrt{(M_x - M_y)^2 + 4M_{xy}^2}} \quad (\text{A1.10a})$$

and

$$\cos 2\alpha = \frac{(M_x - M_y)}{\sqrt{(M_x - M_y)^2 + 4M_{xy}^2}} \quad (\text{A1.10b})$$

Hence, Equation A1.9a becomes,

$$M_n = \frac{(M_x - M_y)}{2} + \frac{1}{2}\sqrt{(M_x - M_y)^2 + 4M_{xy}^2} \quad (\text{A1.11a})$$

Similarly, Equation A1.9b becomes,

$$M_{nt} = 0 \quad (\text{A1.11b})$$

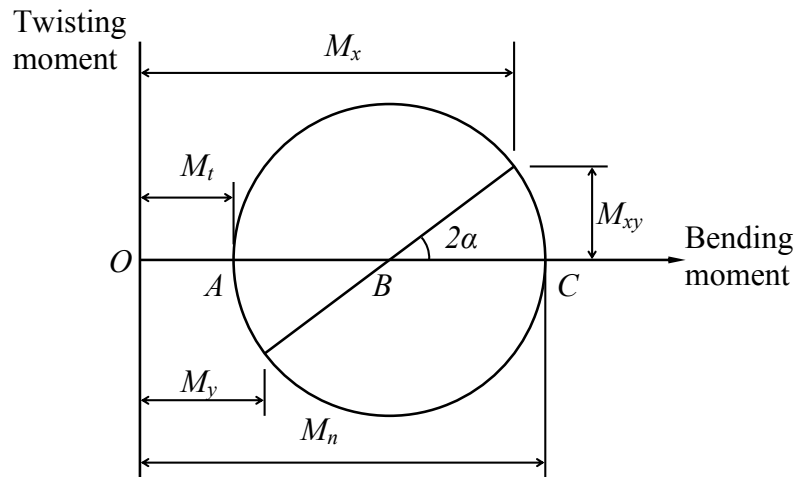


Figure A1. 7 The Mohr's circle presenting the bending moment and twisting moments at a point in a plate

From Figure A1. 7,

$$M_x + M_y = M_n + M_t = 2.0 AB \quad (\text{A1.12a})$$

Also,

$$M_x - M_y = (M_n - M_t) \cos 2\alpha \quad (\text{A1.12b})$$

$$M_{xy} = (M_n + M_t) \sin 2\alpha \quad (\text{A1.12c})$$

Because  $n, t$  are the principal directions ( $M_{nt} = 0$ ), then

$$M_n - M_t = -D(1 - \nu) \left( \frac{\partial^2 w}{\partial n^2} - \frac{\partial^2 w}{\partial t^2} \right) \quad (\text{A1.12d})$$

By simply repeating differentiation and algebraic manipulations, the relationship between twists and curvatures, which are represented by on a Mohr's circle as shown in Figure A1. 8 and the following equations, can be obtained.

$$\frac{\partial^2 w}{\partial x^2} = \frac{1}{2} \left( \frac{\partial^2 w}{\partial n^2} + \frac{\partial^2 w}{\partial t^2} \right) + \frac{1}{2} \left( \frac{\partial^2 w}{\partial n^2} - \frac{\partial^2 w}{\partial t^2} \right) \cos 2\alpha \quad (\text{A1.13a})$$

$$\frac{\partial^2 w}{\partial y^2} = \frac{1}{2} \left( \frac{\partial^2 w}{\partial n^2} + \frac{\partial^2 w}{\partial t^2} \right) - \frac{1}{2} \left( \frac{\partial^2 w}{\partial n^2} - \frac{\partial^2 w}{\partial t^2} \right) \cos 2\alpha \quad (\text{A1.13b})$$

$$\frac{\partial^2 w}{\partial x \partial y} = -\frac{1}{2} \left( \frac{\partial^2 w}{\partial n^2} - \frac{\partial^2 w}{\partial t^2} \right) \sin 2\alpha \quad (\text{A1.13c})$$

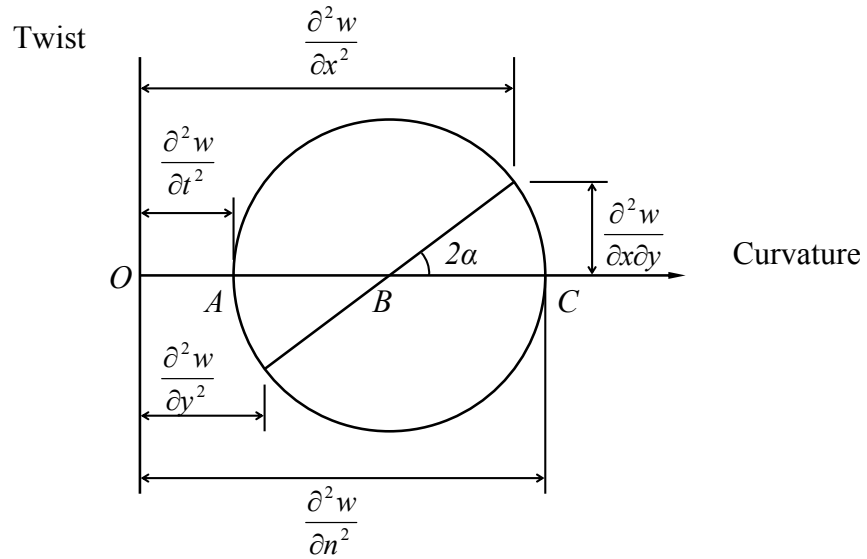


Figure A1. 8 The Mohr's circle presenting twists and curvatures at a point in a plate

From Equations A1.12c, d and A1.13c,

$$M_{xy} = D(1 - \nu) \frac{\partial^2 w}{\partial x \partial y} \quad (\text{A1.14})$$

In addition, Equations A1.12a and b leads to the following equations,

$$M_x = \frac{1}{2}(M_n + M_t) + \frac{1}{2}(M_n - M_t)\cos 2\alpha \quad (\text{A1.15a})$$

$$M_y = \frac{1}{2}(M_n + M_t) - \frac{1}{2}(M_n - M_t)\cos 2\alpha \quad (\text{A1.15b})$$

Adding and subtracting Equations A1.13,

$$\frac{\partial^2 w}{\partial x^2} + \frac{\partial^2 w}{\partial y^2} = \frac{\partial^2 w}{\partial n^2} + \frac{\partial^2 w}{\partial t^2} \quad (\text{A1.16a})$$

and

$$\frac{\partial^2 w}{\partial x^2} - \frac{\partial^2 w}{\partial y^2} = \left( \frac{\partial^2 w}{\partial n^2} - \frac{\partial^2 w}{\partial t^2} \right) \cos 2\alpha \quad (\text{A1.16b})$$

By using Equations A1.8

$$M_n = -D \left( \frac{\partial^2 w}{\partial n^2} + \nu \frac{\partial^2 w}{\partial t^2} \right) \quad (\text{A1.17a})$$

and

$$M_t = -D \left( \frac{\partial^2 w}{\partial t^2} + \nu \frac{\partial^2 w}{\partial n^2} \right) \quad (\text{A1.17b})$$

Substituting Equations A1.17 onto Equation A1.15a, and using the relationship of Equations A1.16

$$M_x = -D \left( \frac{\partial^2 w}{\partial x^2} + \nu \frac{\partial^2 w}{\partial y^2} \right) \quad (\text{A1.18a})$$

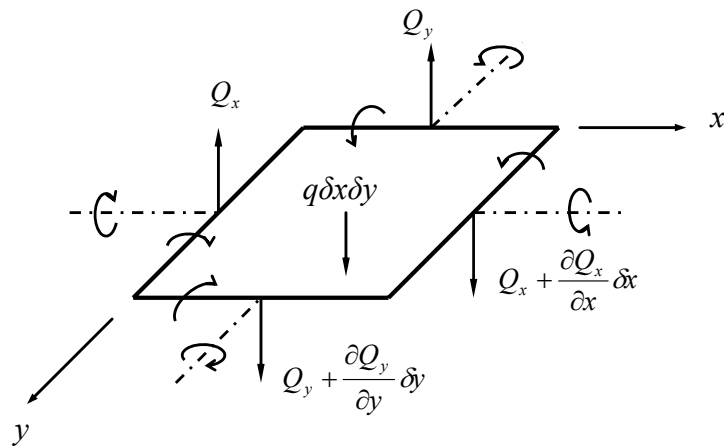
Similarly,

$$M_y = -D \left( \frac{\partial^2 w}{\partial y^2} + \nu \frac{\partial^2 w}{\partial x^2} \right) \quad (\text{A1.18b})$$

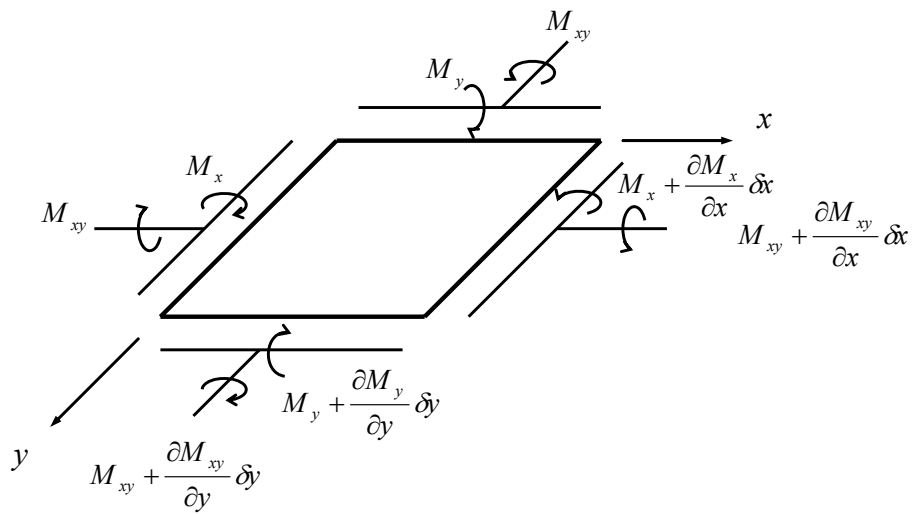
Thus, the following Equations are always true not only in the principal direction but in any direction.

$$\left. \begin{aligned} M_x &= -D \left( \frac{\partial^2 w}{\partial x^2} + \nu \frac{\partial^2 w}{\partial y^2} \right) \\ M_y &= -D \left( \frac{\partial^2 w}{\partial y^2} + \nu \frac{\partial^2 w}{\partial x^2} \right) \\ M_{xy} &= D(1-\nu) \frac{\partial^2 w}{\partial x \partial y} \end{aligned} \right\} \quad (\text{A1.19})$$

Next, the rectangular plate under transverse loading is considered. Figure A1. 9a shows an element  $\delta x \times \delta y$  of the plate on which shear stress per unit length  $Q_x$  and  $Q_y$  etc. are working. The bending and twisting moments acting on the element are also shown in Figure A1. 9b.



(a)



(b)

Figure A1. 9 An element  $\delta x \times \delta y$  of the plate on which shear stress and bending and twisting moments are acting

Taking vertical reaction of the element gives,

$$\left(\frac{\partial Q_x}{\partial x} \delta x\right) \delta y + \left(\frac{\partial Q_y}{\partial y} \delta y\right) \delta x + q \delta x \delta y = 0$$

i.e.

$$\frac{\partial Q_x}{\partial x} + \frac{\partial Q_y}{\partial y} + q = 0 \quad (\text{A1.20})$$

Taking moments about an axis parallel to the  $x$  axis gives,

$$(Q_y \delta x) \delta y - \left(\frac{\partial M_y}{\partial y} \delta y\right) \delta x + \left(\frac{\partial M_{xy}}{\partial x} \delta x\right) \delta y = 0$$

i.e.

$$\frac{\partial M_y}{\partial y} - \frac{\partial M_{xy}}{\partial x} - Q_y = 0 \quad (\text{A1.21a})$$

Similarly about  $y$  axis,

$$\frac{\partial M_x}{\partial x} - \frac{\partial M_{xy}}{\partial y} - Q_x = 0 \quad (\text{A1.21b})$$

Assuming that  $M_x$ ,  $M_y$  and  $M_{xy}$  are related to the deflection  $w$  and substituting Equations A1.19 into above Equations gives,

$$Q_x = -D \left( \frac{\partial^3 w}{\partial x^3} + \nu \frac{\partial^3 w}{\partial x \partial y^2} \right) - D(1-\nu) \frac{\partial^3 w}{\partial x \partial y^2}$$

i.e.

$$Q_x = -D \left( \frac{\partial^3 w}{\partial x^3} + \frac{\partial^3 w}{\partial x \partial y^2} \right) \quad (\text{A1.22a})$$

and similarly

$$Q_y = -D \left( \frac{\partial^3 w}{\partial y^3} + \frac{\partial^3 w}{\partial y \partial x^2} \right) \quad (\text{A1.22b})$$

Substituting for  $Q_x$  and  $Q_y$  in Equation A1.20 from Equations A1.22,

$$\frac{\partial^4 w}{\partial x^4} + 2 \frac{\partial^4 w}{\partial x^2 \partial y^2} + \frac{\partial^4 w}{\partial y^4} = \frac{q}{D} \quad (\text{A1.23})$$

Equation A1.23 is the governing equation of the rectangular plate under transverse loading  $q$  per unit area.

